André-Henri Dargelas (ca. 1860)

PHENIX Beam Use Proposal Run-14 and Run-15

Submitted May 28, 2013

Executive Summary

The PHENIX Collaboration has a targeted set of physics goals for Run-14 and Run-15 which are enabled by key detector upgrades and new capabilities from the RHIC accelerator. The specific beam use request is documented in terms of recorded or trigger sampled integrated luminosity by the PHENIX experiment within a specific z-vertex window, with our best estimate of the number of weeks required to reach that goal following the C-AD guidance [1]. The beam use proposal charge (included as Appendix A) requested plans for 22 cryo-weeks and alternatively 15 cryo-weeks in both Run-14 and Run-15. The PHENIX collaboration request is as follows.

Run-14 Proposal (22 cryo-weeks)

- Au+Au @ 200 GeV for 12 weeks [Physics driven goal is 1.5 nb^{-1} recorded within $|z| < 10$ cm]
- p+p @ 200 GeV with longitudinal polarization for 6.5 weeks [Physics driven goal is 30 pb^{-1} sampled within $|z| < 30$ cm and $\langle \mathcal{P} \rangle = 60\%$]

Run-14 Proposal (15 cryo-weeks)

- Au+Au @ 200 GeV for 11.5 weeks [Physics driven goal is 1.5 nb^{-1} recorded within $|z| < 10$ cm]

The aim of the Run-14 Au+Au @ 200 GeV request is to collect our definitive heavy ion Au+Au data set for heavy quarks with both forward and barrel silicon detectors and the high RHIC luminosity. The Run-14 p+p @ 200 GeV request provides critical baseline measurements of heavy quark production. Heavy quarks as a probe of thermalization and energy loss have only grown more interesting with recent measurements at RHIC and the LHC. In addition, the p+p @ 200 GeV with longitudinal polarization will further constraint the gluon contribution to the proton spin, where current results indicate for the first time a non-zero gluon contribution [2]. In the case of a restricted 15 cryo-weeks running period, only the Au+Au request can be accommodated. For Run-15 there is a

request for p+p @ 200 GeV with transverse polarization that is higher priority than the p+p @ 200 GeV longitudinal polarization running, and thus a short Run-14 likely results in a loss of these additional gluon spin contribution constraints.

Run-15 Proposal (22 cryo-weeks)

- p+p @ 200 GeV with transverse polarization for 9 weeks [Physics driven goal is 50 pb^{-1} recorded within $|z| < 40$ cm and $\langle \mathcal{P} \rangle = 60\%$]
- p+Au @ 200 GeV with transverse polarization of the proton for 4 weeks [Physics driven goal is 150 nb^{-1} sampled within $|z| < 40$ cm and $\langle \mathcal{P} \rangle = 60\%$]
- Geometry studies with d+Au @ 200 GeV and ^{3}He+Au @ 200 GeV for 1 week each [Physics driven goal is recording 1 billion minimum bias events for each]
- p+Si, p+Cu @ 200 GeV for 2 weeks each [Physics driven goal is 450 nb^{-1} and 225 nb^{-1}, respectively, sampled within $|z| < 40$ cm and $\langle \mathcal{P} \rangle = 60\%$]

Run-15 Proposal (15 cryo-weeks)

- p+p @ 200 GeV with transverse polarization for 7 weeks [Physics driven goal is 30 pb^{-1} recorded within $|z| < 40$ cm and $\langle \mathcal{P} \rangle = 60\%$]
- p+Au @ 200 GeV with transverse polarization of the proton for 4 weeks [Physics driven goal is 150 nb^{-1} sampled within $|z| < 40$ cm and $\langle \mathcal{P} \rangle = 60\%$]

For Run-15 the highest priority is to obtain a substantial data set of transversely polarized p+p @ 200 GeV and p+Au @ 200 GeV, with the proton transversely polarized. The proposed Run-15 request is aggressive in terms of the assumed switching time between colliding species as there are numerous exciting physics topics accessed by the unique geometry and polarization capabilities of RHIC. The priority ordering of the request after p+Au will be significantly informed by theoretical and experimental results over the next year.

For Run-15, we are on schedule to have the MPC-EX upgrade detector complete and ready for physics. The MPC-EX enables the measurement of direct photons and extends the kinematic coverage for neutral pions at very forward rapidity. The length of the request for p+p @ 200 GeV with transverse polarization is driven by the measurement of the direct photon A_N with the MPC-EX, open charm A_N with the silicon vertex detectors, in addition to important baseline measurements for comparison with p+A results. There is enormous excitement in the collaboration for utilizing the new capability for running polarized p+A with a short switchover time as enabled by stochastic cooling [1]. For example, new measurements with the MPC-EX will utilize new theoretical tools for probing gluon saturation physics with transverse polarization measurements.

In addition, testing the geometric dependence of many key observables (including heavy quarks, heavy quarkonia, jets, and flow observables) in p+Si, p+Cu, p+Au is a high priority. The unique ability of RHIC is highlighted in our request for a short d+Au and ^{3}He+Au run, where one can directly compare with the PHENIX full suite of correlation measurements the different geometries of p+Au, d+Au, and ^{3}He+Au where one selects for intrinsically larger ε_2 and ε_3 for the latter two combinations respectively.

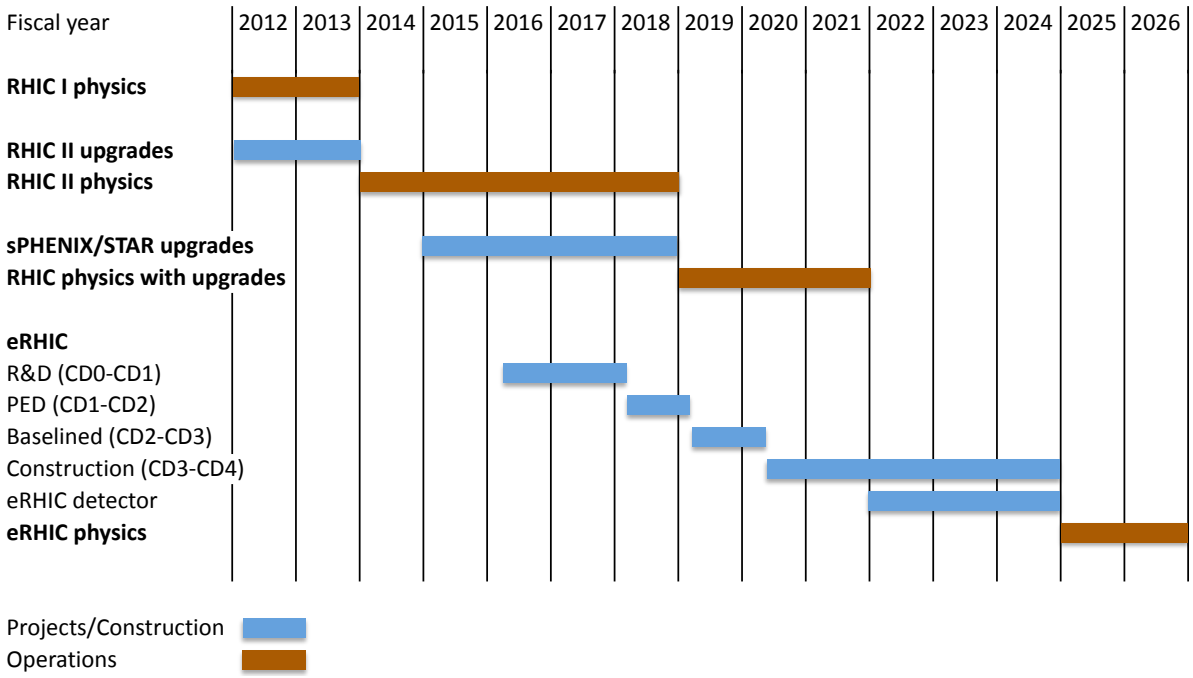

Figure 1: Official BNL timeline through the mid-2020s, including a transition to eRHIC.

The collaboration's highest priority for Run-13 was to complete the longitudinally polarized p+p @ 500 GeV W physics program. At the time of this writing it is clear that the full luminosity and polarization goals will not be fully achieved. The collaboration remains very interested in obtaining the best constraint on the (anti) up, (anti) down quark spin contributions and will revisit the question of additional requested p+p @ 500 GeV longitudinally polarized data when at least a preliminary version of the Run-13 results are available.

Our beam use request is significantly informed by the overall timeline for running at RHIC and the broader PHENIX upgrade program of sPHENIX and an evolution to a dedicated Electron Ion Collider detector, ePHENIX. The current schedule being used by the Laboratory is shown in Figure 1. PHENIX has a major detector upgrade plan, sPHENIX, which was reviewed in October 2012 and the review committee "strongly endorsed the science case for this program." The MIE Proposal [3] has been officially submitted to the Department of Energy and awaits CD-0 approval. If successful, PHENIX would require a one-year shutdown for sPHENIX installation in the time frame of 2017 to 2019. Thus, the PHENIX collaboration views the next three years of running as requiring sufficient

luminosity to make definitive measurements with the excellent detector capabilities and accelerator performance available now.

The PHENIX collaboration has a strong interest in the possible future Electron Ion Collider and has documented an evolution fully utilizing the PHENIX infrastructure and sPHENIX upgrades for transforming into a world-class ePHENIX detector, as shown in Figure 2.

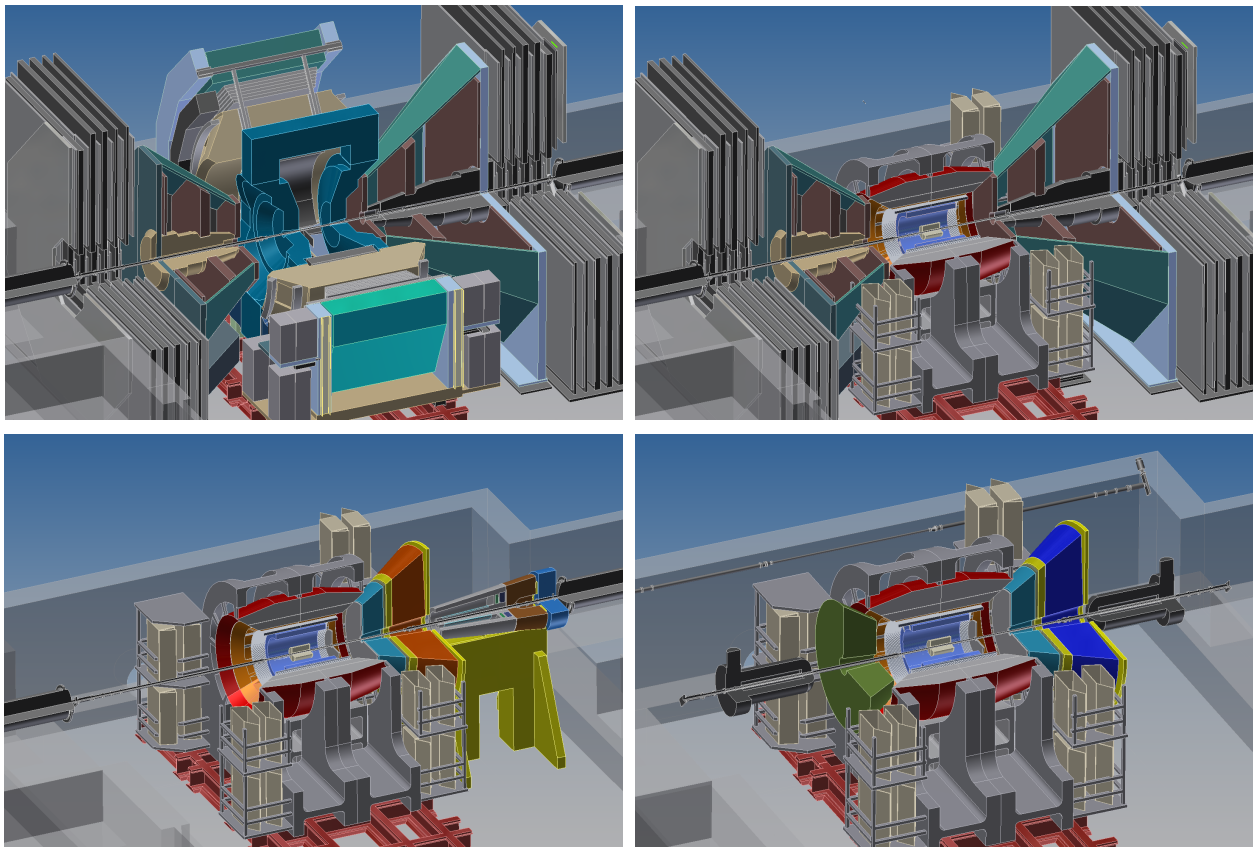

Figure 2: Engineering renderings for the evolution of PHENIX. Upper left is the current PHENIX detector. Upper right is the proposed sPHENIX in the MIE. Lower left includes additional upgrades at forward angles. Lower right is ePHENIX for the Electron Ion Collider physics.

Contents

Chapter 1

Recent scientific accomplishments

The PHENIX collaboration has produced a set of highly impactful results this past year, including the completion of promised measurements along with some unexpected new results. A strong theme amongst the results is the utilization of the unique flexibility of RHIC and the continued implementation of new PHENIX detectors and analysis techniques.

1.1 Cold nuclear matter results

We are making a big push to complete all cold nuclear matter data analysis from the excellent Run-08 d+Au data set, as it has timeliness with the LHC p+Pb running and looking forward to the new RHIC capabilities for polarized p+A. Utilizing the upgrade project MRPC time-of-flight west detector, we have submitted for publication the identified π, K, p transverse momentum spectra in centrality categories for d+Au and Au+Au [4]. These comprehensive results as shown in Figure 1.1 show a striking similarity of the baryon anomaly (enhanced baryon to meson yields at intermediate transverse momentum) for central d+Au and peripheral Au+Au, thus challenging many theoretical interpretations that require higher parton densities.

Most recently the PHENIX collaboration has asked the question of whether the long range correlation phenomena seen in very high multiplicity p+p and p+Pb collisions at the LHC is also occurring at RHIC energies and with the unique geometry of d+Au collisions [5]. Shown in the left panel of Figure 1.2 is a calculation of the initial distribution of deposited energy in a MC-Glauber scenario from B. Schenke *et al.* [6]. The right panel of the same figure shows the PHENIX extracted v_2 coefficients as a function of transverse momentum compared with four different hydrodynamic simulations with different initial geometry and viscosity assumptions. In Figure 1.3, we show that the significant elliptic flow component extends over a very wide rapidity gap with preliminary measurements utilizing the forward MPC calorimeter. The collaboration is excited to follow these measurements

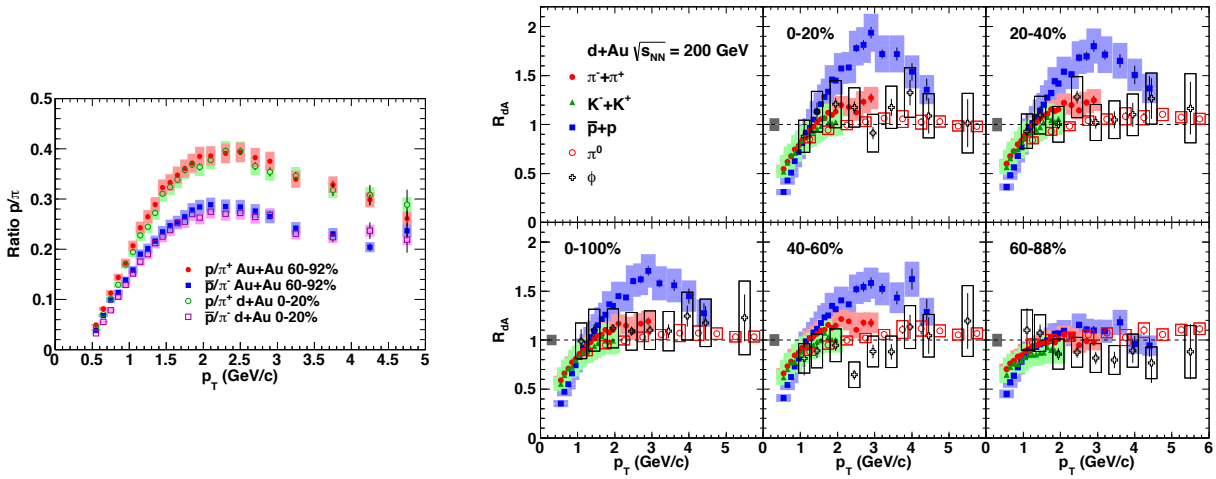

Figure 1.1: (left) Ratio of p/π^+ and $\overline{p}/\pi^-$ as a function of transverse momentum in central d+Au and peripheral Au+Au where the number of participating nucleons is similar. (right) The nuclear modification factor, R_{dAu}, for different d+Au centrality selections where the emergence of the baryon anomaly is seen.

with different manipulations of the initial geometry, as detailed in this beam use proposal.

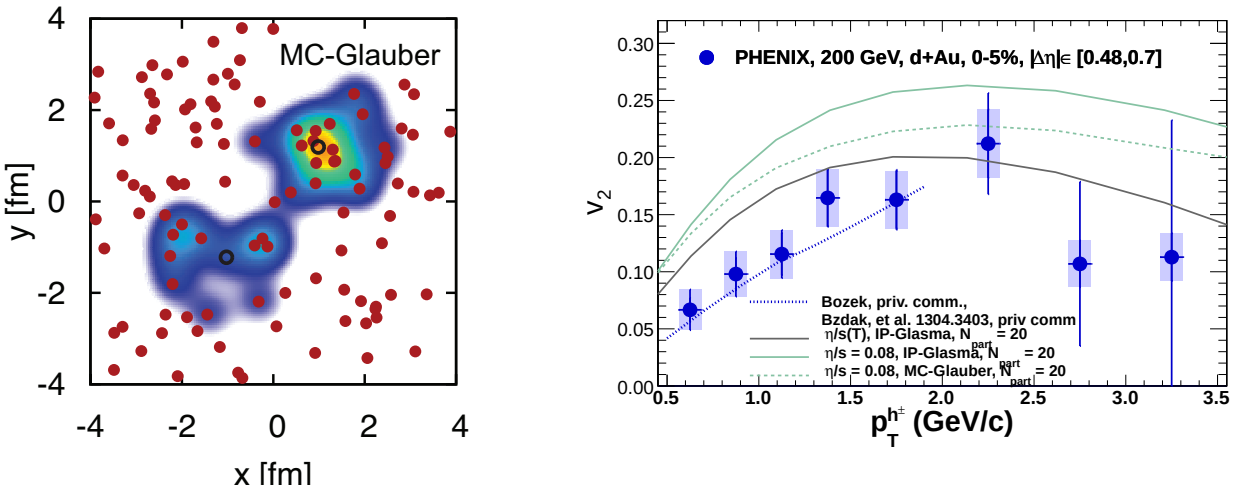

Figure 1.2: (left) Energy deposition distribution for a single d+Au @ 200 GeV event from Bjoern Schenke in the MC-Glauber framework [6]. (right) PHENIX extraction of v_2 coefficients as a function of transverse momentum for very central d+Au collisions. Shown for comparison are various hydrodynamic calculations with different initial geometry and viscosity assumptions [6, 7].

In addition, the PHENIX experiment has published a suite of our d+Au results with interesting implications for nuclear modified parton distribution functions and interactions with cold nuclear matter. These include the nuclear modification factor R_{dAu} of J/ψs [8], Upsilons [9], direct photons [10], and open heavy flavor measured via single leptons [11].

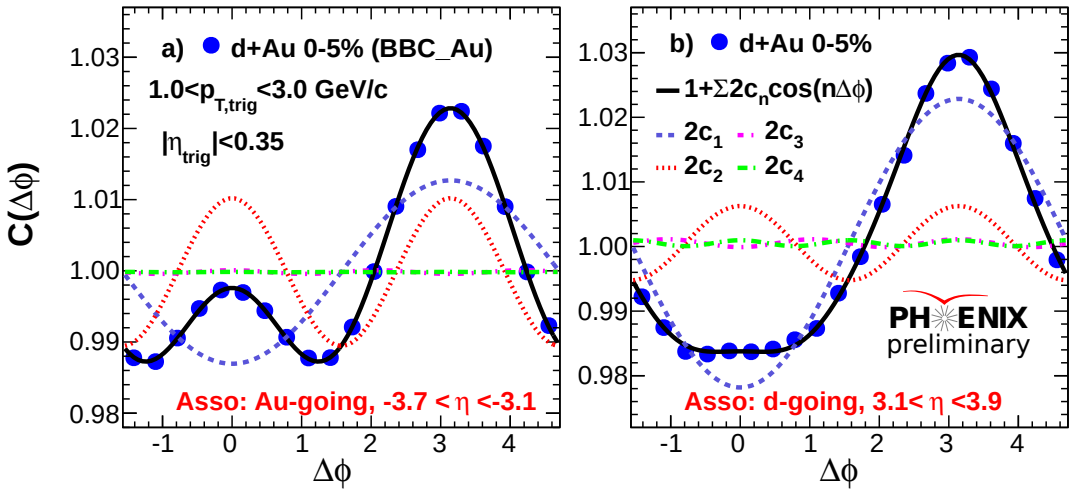

Figure 1.3: Plotted is the correlation function in central d+Au @200 GeV collisions between central arm tracks (CNT) at midrapidity with p_T = 1.0–3.0 GeV/c with energy deposited in the MPC calorimeter covering pseudorapidity -3.0 to -3.8 (Au going direction) and +3.0 to +3.8 (d going direction) in the left and right panels respectively.

Figure 1.4 shows the open heavy flavor results from single electrons and muons as a function of d+Au centrality. One observes a clear enhancement in the Au-going direction sensitive to high-x partons in the anti-shadowing regime and suppression in the d-going direction sensitive to low-x partons in the shadowing regime. Connecting this physics more directly to nuclear modified parton distributions requires separation of charm and beauty contributions in future running with the PHENIX silicon vertex detector upgrades and direct photon measurements enabled by the MPC-EX upgrade.

Another interesting result is the stronger suppression of the ψ' compared to the J/ψ in the more central d+Au collisions as shown in Figure 1.4. These measurements set an important baseline for hot nuclear matter effects in Au+Au collisions, and an interesting challenge for theoretical calculations to simultaneously explain this suppression as well as the least bound Upsilon state as already measured at the LHC.

An intriguing result presented this last year is the nuclear modification factor for high transverse momentum neutral pions and fully reconstructed jets. The results shown in Figure 1.5 indicate a significant enhancement in peripheral d+Au events and a modest suppression in the most central d+Au events. The question remains outstanding whether competing cold nuclear matter effects may explain the data, or there are important auto-correlations between these high transverse momentum processes and the centrality determination. Further data with p+A collisions with light ions can elucidate the answer as they have similar number of binary collisions as peripheral d+Au and without the need for centrality selection.

Many of these results raise good scientific questions and can be substantially advanced

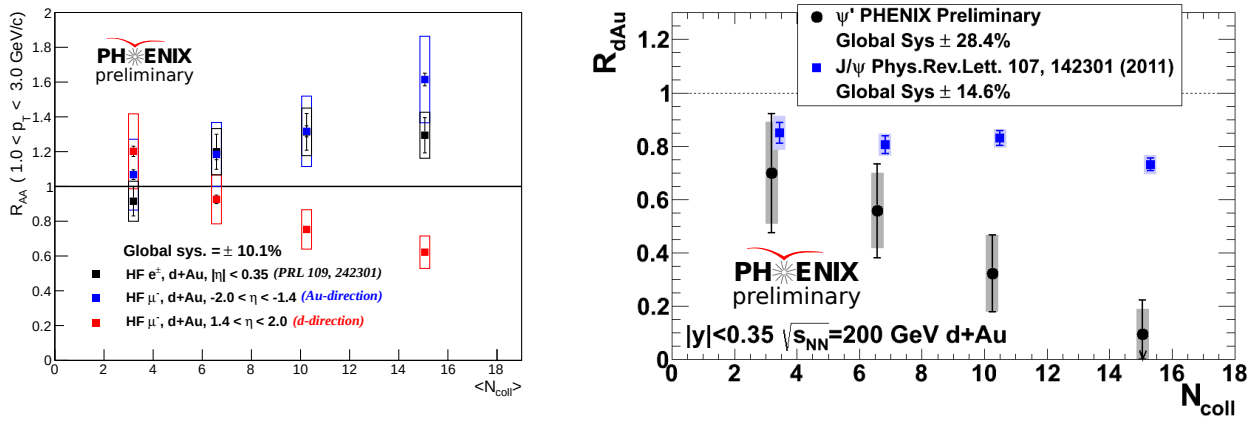

Figure 1.4: (left) The nuclear modification factor in d+Au collisions for open heavy flavor measured via single electrons and muons. (right) The nuclear modification factor in d+Au collisions for the J/ψ and ψ'.

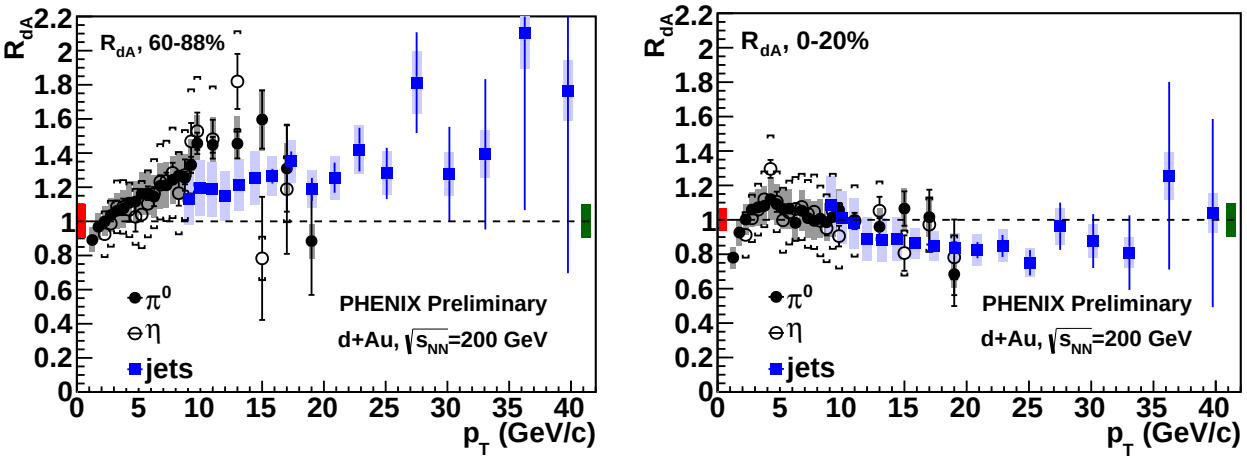

Figure 1.5: R_{dAu} for π^0s, ηs and fully reconstructed jets in peripheral (left) and central (right) collisions.

through p+A running and with the new PHENIX detector capabilities available for Run-15. In particular the synergy between RHIC and the LHC results is critical for assessing competing theoretical explanations involving Color Glass Condensate glasma diagrams and collective hydrodynamics coupled to the initial geometry, pinning down the nuclear parton distribution functions particularly for gluons, and understanding other mechanisms such as initial state parton energy loss. RHIC is ideally suited to advance this scientific process of making theoretical predictions for discriminating observables and then measuring them.

1.2 New geometry studies with Cu+Au and U+U

The PHENIX experiment collected excellent data sets in Run-12 with new geometry configurations of Cu+Au and U+U @ 200 GeV. Preliminary results were shown at the QM'12 conference last year that highlight the utility of these systems. For instance, a full suite of flow measurements have also been made in Cu+Au, including the v_1 and v_2 coefficients as a function of transverse momentum, as shown in Figure 1.6. These results have the opposite sign of v_1 at midrapidity compared with AMPT model predictions, which may be due to a different shift in the center-of-mass of the medium.

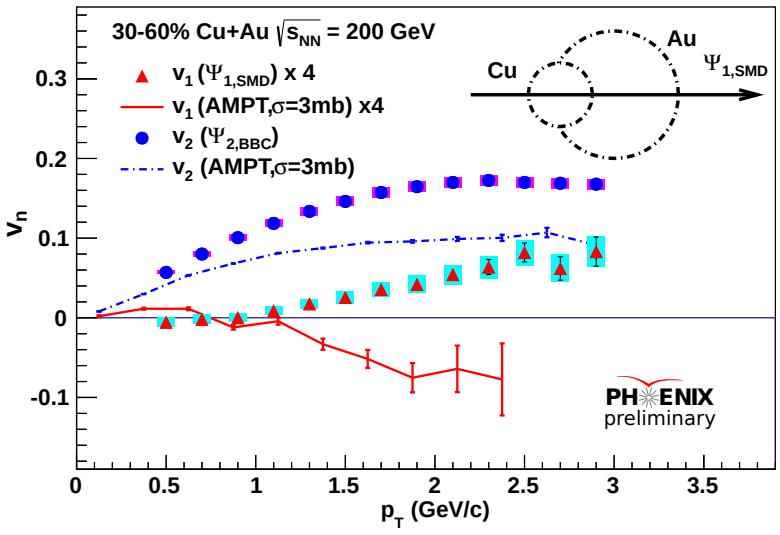

Figure 1.6: Cu+Au flow coefficients v_1 and v_2 as a function of transverse momentum compared with AMPT model calculations.

We have characterized the charged particle multiplicity and energy density in U+U collisions. In selecting up to the one percent most central events, one reaches more than 6 GeV/fm^3 at a time of 1 fm/c, as shown in Figure 1.7. Interesting flow results have also been reported, indicating a possible increase in radial flow in the most central events. Studies on the selection of particular geometries related to the oblate initial nuclear geometry are underway and results already indicate that particle multiplicities do not follow a simple $x \times N_{\text{part}} + (1-x) \times N_{\text{coll}}$ relation.

1.3 Photons, dileptons, and open heavy flavor

The PHENIX collaboration has submitted for publication a set of direct photon-hadron correlation results that reveal a significant suppression of direct photon correlated hadrons at high z_T [12], presumably due to jet quenching. In addition, the angular distribution

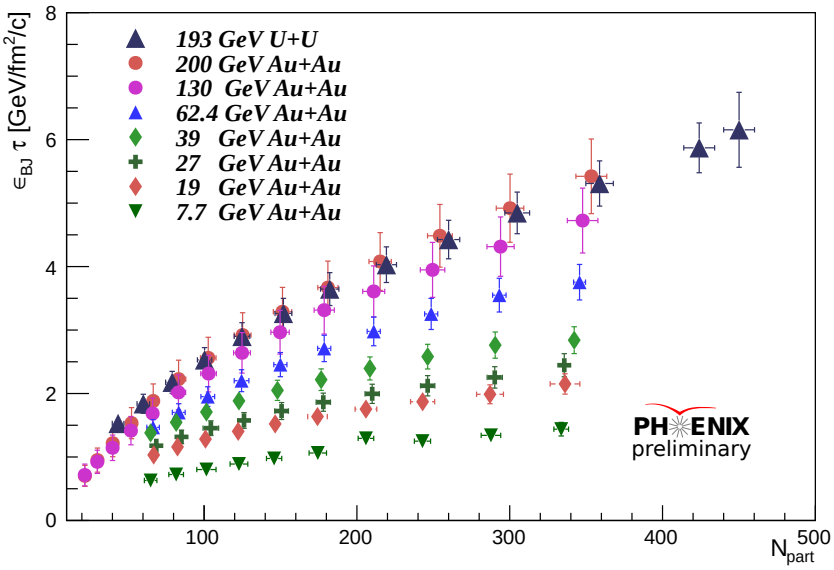

Figure 1.7: Bjorken energy density times time as a function of number of collision participants for various collision species and energies. The U+U data is selected up to the one percent most central event category.

of low momentum correlated hadrons reveals a redistribution of lost energy over a wide cone almost the size of a full hemisphere as shown in Figure 1.8.

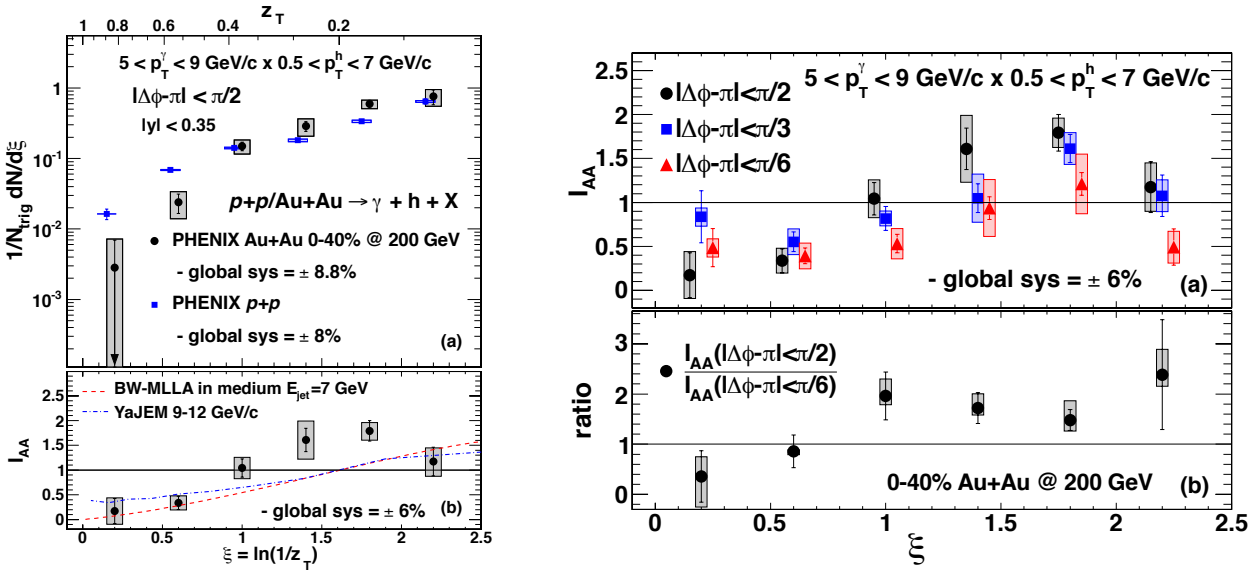

Figure 1.8: (left) Per trigger yield and I_{AA} for hadrons correlated with direct photons. A clear suppression at high z (or low ξ) is observed. (right) The I_{AA} for different angular selections reveals an enhanced correlated yield at large angles.

The PHENIX collaboration has made progress towards publication of the Run-10 Au+Au dilepton results with the Hadron Blind Detector. Preliminary results were shown for peripheral and midcentral events. The status of the central Au+Au results and finalizing the entire analysis for publication is presented in Section 2.5.

Run-11 was the commissioning run of the PHENIX silicon vertex barrel detector (VTX). These results have relatively low statistics and the detector had a limited geometry due to a number of now understood issues. Preliminary results in p+p collisions shown in Figure 1.9 indicate good agreement with the charm to beauty fraction for electrons with previous results calculated via electron-hadron correlations [13] and FONLL calculations. Preliminary Au+Au results were shown [14] and afterwards it was determined that important systematic uncertainties due to the uncertainty in the B meson parent transverse momentum distribution were not properly taken into account. The PHENIX collaboration is focused on producing final results for publication in the next six months. Details on the detector readiness for Run-14 are included in Section 2.2.

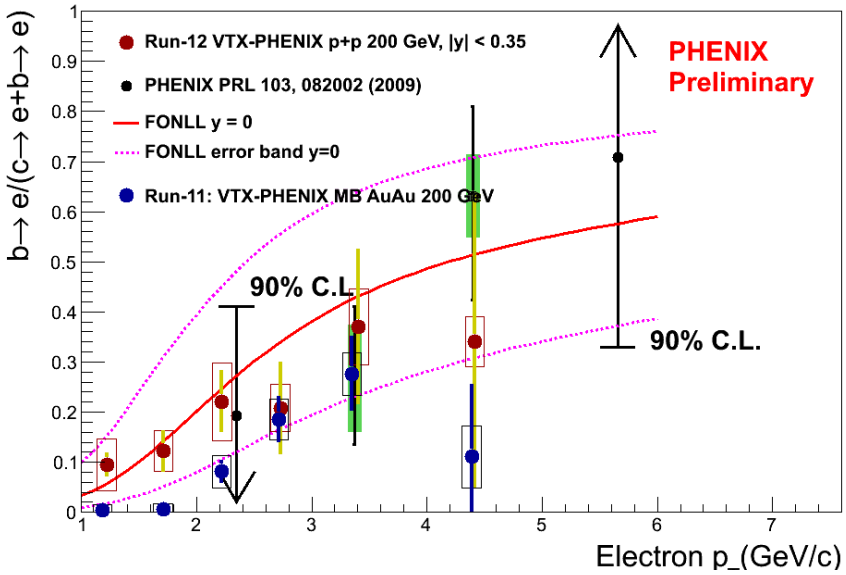

Figure 1.9: Charm and beauty contribution separation via electrons with displaced vertices with the PHENIX VTX detector. The results are compared with results from electron-hadron correlations [13] and FONNL calculations.

1.4 Spin physics results

The PHENIX experiment has high statistics neutral pion double spin asymmetries A_{LL} from the combined Run-05, Run-06, Run-09 data sets, which when considered with the STAR experimental results on reconstructed jets, give the first indication of a non-zero gluon contribution to the proton spin [2]. The preliminary A_{LL} results and the global

DSSV++ fits are shown in Figure 1.10. The PHENIX collaboration has finalized these results and expects to submit them for publication soon. The Run-14 request for additional longitudinally polarized $p+p$ @ 200 GeV can significantly improve on the constraint from gluon contributions at low-x.

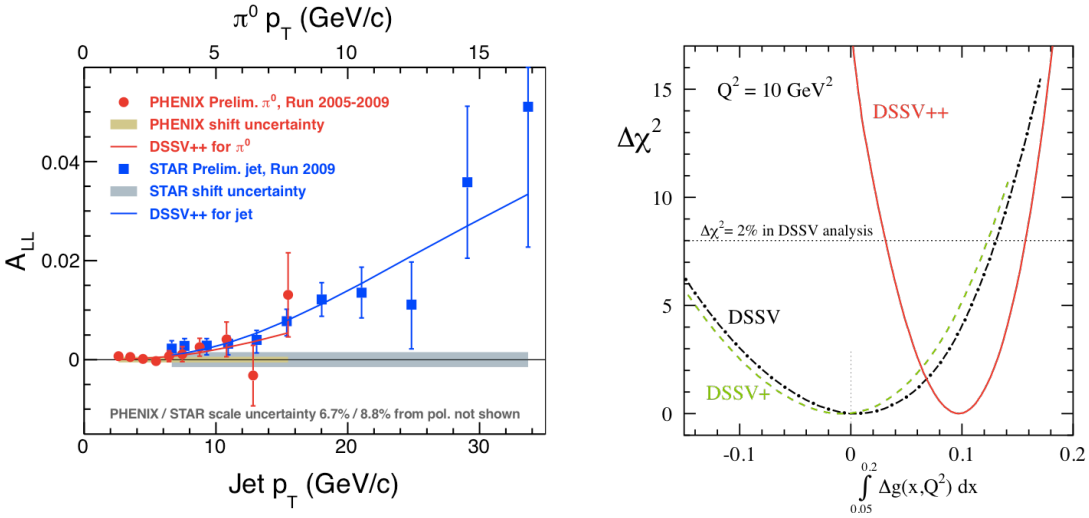

Figure 1.10: (left) PHENIX and STAR double spin asymmetries for neutral pions and jets respectively. (right) DSSV++ global constraint fit on the gluon spin contribution over the finite x range 0.05 to 0.2.

Significant progress has been made on the analyses of $W \rightarrow e$ at midrapidity and $W \rightarrow \mu$ at forward rapidity. Shown in Figure 1.11 are preliminary results from Run-09 $p+p$ @ 500 GeV results at midrapidity. The collaboration expects to publish these results soon and looks forward to analyzing the highest statistics results from the combined data sets including the now running Run-13 results.

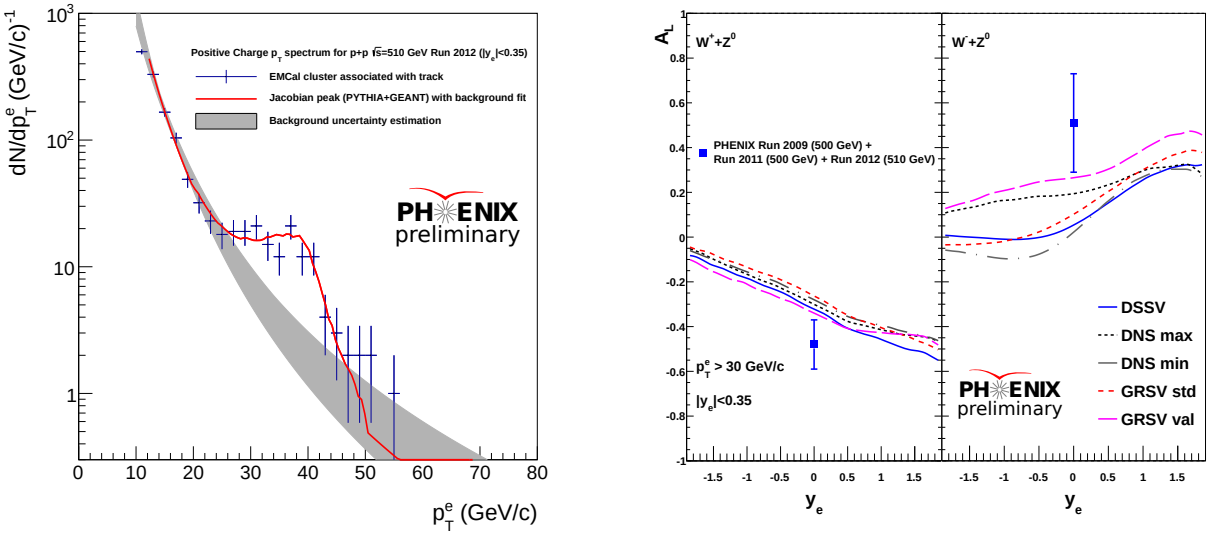

Figure 1.11: (left) Transverse momentum distribution for midrapidity electrons with a clear peak from the W boson contribution. (right) Single spin asymmetries for W^+ and W^- contributions compared with various calculations.

Chapter 2

Status of upgrades

In this Chapter we report on the status of key PHENIX detector upgrade projects. The first three relate to the forward silicon vertex detector (FVTX), the barrel silicon vertex detector (VTX), and the Muon Piston Calorimeter Extension upgrade (MPC-EX). These three projects are directly relevant to the physics measurements and readiness for the proposed data taking in Run-14 and Run-15 of this beam use proposal. Then we detail the successful implementation and running of the Muon Trigger and Resistive Plate Chamber (RPC) upgrade for the spin W physics program as utilized in $p+p$ @ 500 GeV running this past Run-13. We then give a status report on the Hadron Blind Detector (HBD) which completed data taking in Run-10 before being removed for installation of the silicon vertex detectors. Finally we have a brief update on a few smaller scale and very successful upgrades – the time-of-flight west MRPC detector and the data acquisition and trigger improvements.

2.1 Forward silicon vertex detector (FVTX)

The PHENIX detector Barrel and Forward Silicon Vertex Trackers are shown in Figure 2.1. The two Forward Silicon Vertex Trackers (FVTX) are endcap detectors which extend the vertex capability of the VTX to forward and backward rapidities, providing space points before the absorber materials and secondary vertex measurement capability in front of the PHENIX muon arms. The FVTX detector was successfully installed into PHENIX in December 2011 and has undergone commissioning and operations during Run-12 and Run-13. During the shutdown following Run-12, $\sim$ 10% of the FVTX electronics were repaired and FPGA code was updated, resulting in a detector which has been $>$ 95% operational for Run-13.

The FVTX was designed to be able to identify secondary vertices near the primary event vertex. With an expected distance of closest approach (DCA) resolution of better than

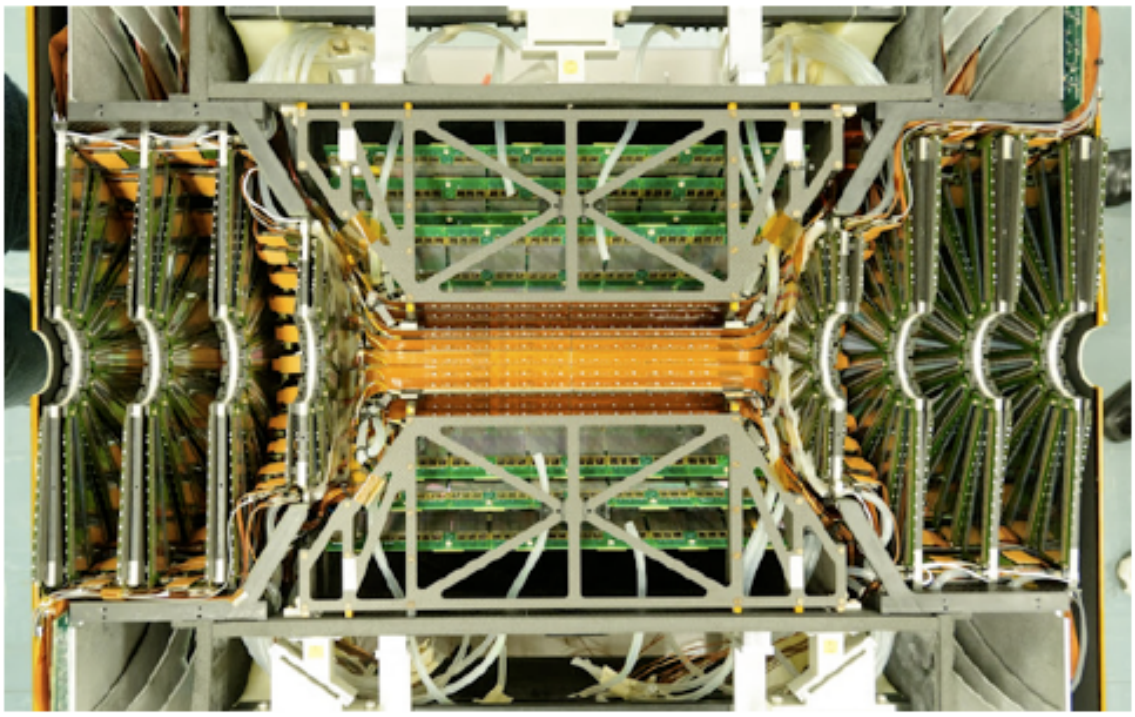

Figure 2.1: VTX Barrel plus FVTX end cap.

200 μm at 5 GeV/c, we can separate prompt particles from particles that have short decay distances (B and D mesons) and longer-lived particles such as pions and kaons. The FVTX detector improves the dimuon mass resolution by providing a better opening angle measurement than can be provided by the muon arms alone, allows for isolation cuts to help discriminate between muon signals and hadronic backgrounds, and will provide further discrimination against hadronic particles which decay in the muon volume by requiring that the track passing through the FVTX planes and the muon planes have a good χ^2 fit value. With these new capabilities, we can precisely measure open heavy flavor production at forward rapidity, improve the background rejection and separation of J/ψ and ψ' in the dimuon spectra, and separate Drell-Yan dimuons from dimuons produced through heavy flavor and/or hadronic decays. The FVTX detector also improves the reaction plane measurement significantly. The FVTX is also providing a new precision measurement of the relative bucket-to-bucket luminosities in polarized p+p collisions, which is critical for PHENIX spin analyses.

In Run-12, the intrinsic performance of the FVTX detector was studied using real collision data and front-end injection calibration data, and all detector performance specifications were met, including >95% detector efficiency in the active area, ~500 electrons noise level on all readout channels, and an intrinsic detector resolution limited only by the readout pitch and multiple scattering of particles. Since then, we have analyzed Run-12

and early Run-13 data and studied the track finding efficiencies, the DCA performance, the improvement to the dimuon mass resolution, the background rejection and the reaction plane resolution. Figure 2.2 shows the reconstructed dimuon mass in the J/ψ region for a set of Run-13 runs for the muon arm alone (red) and, for the same data set, the combined muon and FVTX detector mass spectrum (blue crosses). Both histograms have been re-scaled. As can be seen, the FVTX improves the mass resolution significantly and the combinatorial background is reduced.

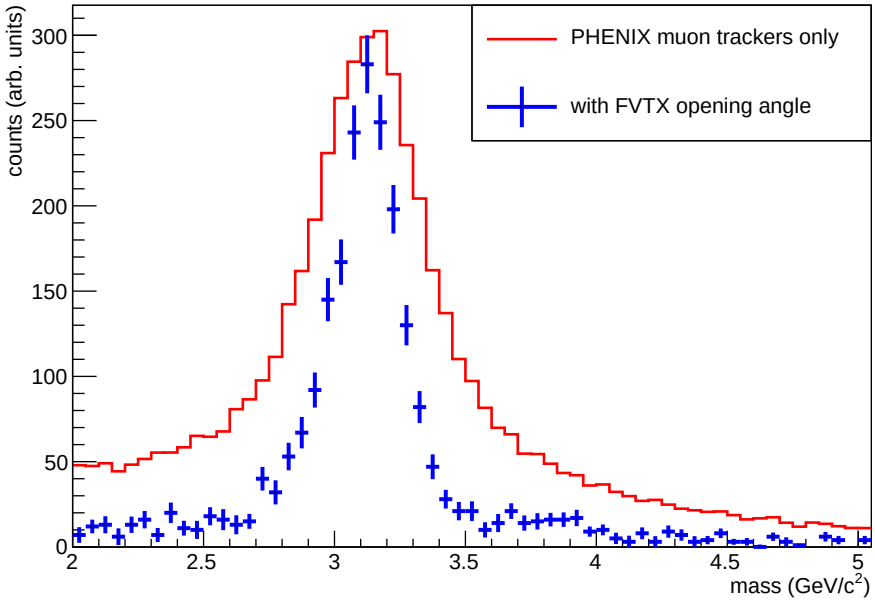

Figure 2.2: Reconstructed dimuons in the J/ψ mass region for a set of the Run-13 $p+p$ data. Shown in red is the reconstructed mass from the muon arm alone and the blue crosses show the reconstructed mass for tracks which are matched to FVTX tracks and refit using the FVTX detector. Both histograms have been re-scaled.

The FVTX detector is ready for definitive open heavy flavor measurements in Au+Au and $p+p$ in Run-14.

2.2 Barrel silicon vertex detector (VTX)

The PHENIX Silicon Vertex Tracker (VTX) is a 3.5M channel device consisting of two inner pixel layers and two outer stripixel layers arranged in a barrel geometry in close proximity to the beryllium beam pipe. The VTX shares a mechanical support structure, cooling and electrical services with the Forward Silicon Tracker (FVTX) which consists of two end caps each containing four planar disks of silicon pads. The VTX was completed in the late fall of 2010 and installed in the PHENIX IR for an engineering run during the RHIC 2011 run

(Run-11). Initial commissioning of the VTX in early 2011 identified numerous problems with unreliable readout electronics in both the pixel and stripixel readout chains that had not been apparent during QA and bench testing of the electronics boards. However through dedicated commissioning efforts the VTX was integrated into PHENIX and took physics data during the final 6–8 weeks of Run-11 with 70–75% live channels.

Repairs and modifications to various VTX electronics boards took place beginning in the 2011 RHIC summer shutdown in preparation for Run-12. Once the electronics were repaired and reinstalled it was discovered that approximately 20–25% of on-board pixel readout chips that had been working at the beginning of Run-11 were no longer operational. Investigations determined that this was due to failures of the wire bonds connecting the chips to the readout buses. Studies by BNL, RIKEN and the wire bonding company Hayashi showed that the pixel wire bonds were unusually sensitive to thermal stresses from temperature cycling of the VTX during typical detector operations. No similar effects were observed in the stripixel wire bonds. A number of steps were taken to greatly reduce the pixel wire bond losses and prevent future recurrence. The VTX cooling system was reconfigured and operating procedures changed to reduce temperature changes in the VTX pixel ladders and prevent periods of rapid cool down and warm up. In addition a multi-year program to rebond the sensors was initiated. The rebonding also includes a change in the epoxy encapsulant to one that imposes less mechanical stress on the bonds.

The VTX took physics data in the 2012 RHIC run with approximately 80% live channels. VTX maintenance activities during the 2012 shutdown included the repair of a small number of electronics boards and the continuing replacement of pixel ladders with bonding problems with newly rebonded ladders. Unfortunately during VTX commissioning prior to the start of the 2013 RHIC run, a number of coolant leaks were detected in the VTX stripixel ladders. A detailed investigation identified the cause of the leaks as galvanic corrosion due to an interaction between the aluminum cooling tube and surrounding carbon fiber foam in the stripixel stave. It is likely that water condensation helped to speed the corrosion process. The leaks were so wide-spread and the observed corrosion so advanced that it was decided just prior to the start of Run-13 to remove 1/2 the VTX detector from the IR and bypass the stripixel staves that remain installed in PHENIX. Only the west half of the VTX pixel layers is active during the RHIC 2013 run.

Since the corrosion was discovered we have redesigned the stripixel staves, replacing the aluminum tubes used to carry the coolant with PEEK plastic-carbon composite conduits—very similar to the design working successfully in the FVTX. We have initiated a plan to replace all 40 VTX stripixel staves between now and the start of the 2014 RHIC run. In addition 15 pixel ladders are having their wire bonds replaced in Japan and are scheduled to be shipped to BNL starting in early June 2013. We are working to a plan that will have the VTX fully reconstructed with $\geq$ 95% live channels in time for a January 1, 2014 cool down of RHIC.

2.3 Muon piston calorimeter extension (MPC-EX)

The Muon Piston Calorimeter (MPC) Extension, or MPC-EX, is a Silicon-Tungsten preshower detector that will be installed in front of the existing PHENIX MPCs, as shown in Figure 2.3. This detector consists of eight layers of Si "minipad" sensors interleaved with tungsten absorber and enables the identification and reconstruction of prompt photons and π^0s at energies up to $\sim$ 80 GeV.

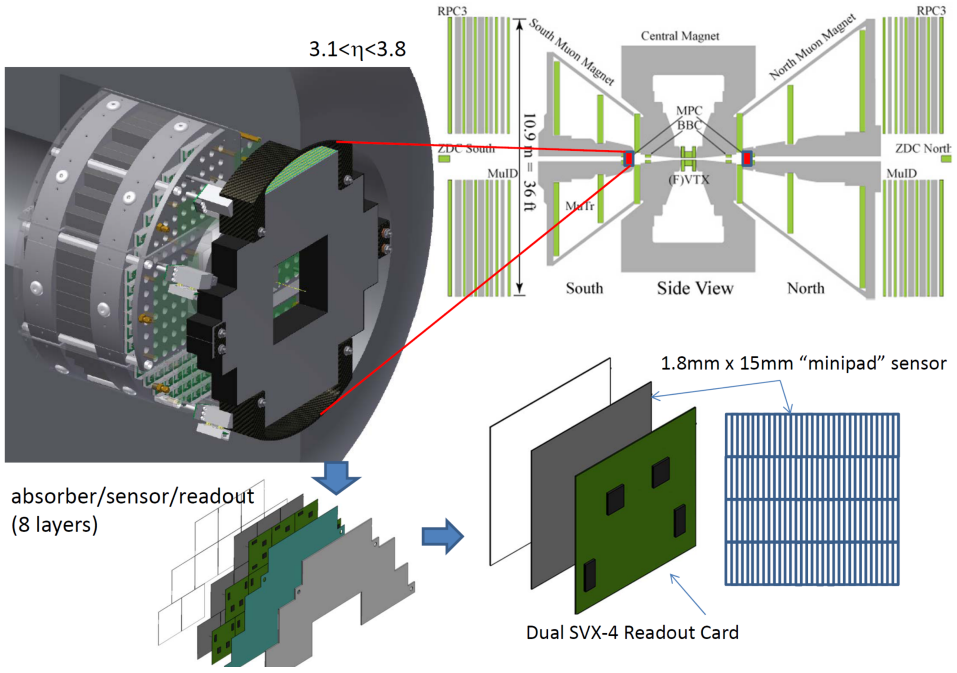

Figure 2.3: The PHENIX detector (upper right), showing the location of the existing Muon Piston Calorimeters inside the muon magnet piston. The MPC-EX (upper left) will consist of eight measurement layers of absorber, sensors and readout. The "minipad" sensors themselves (lower right) will consist of a readout card bonded to a Si sensor. The orientation of the long direction of the minipads will alternate between layers.

The MPC and MPC-EX sit at forward and backward rapidities ($3.1 < |\eta| < 3.8$) and are uniquely positioned to measure phenomena related to either low-x partons (in the target hadron or nucleus) or high-x partons (in the projectile nucleon or nucleus). We propose to use the capabilities of the MPC-EX to make critical new measurements that will elucidate the gluon distribution at low-x in nuclei as well as the origin of large transverse single spin asymmetries in polarized p+p collisions. The MPC-EX construction effort and schedule are on track to have a partial installation available for systems integration testing in Run-14, and a full installation in both arms for Run-15.

The active elements in the MPC-EX are the Si minipad sensors. The sensors are 500 μm thick and 6.2 cm $\times$ 6.2 cm in size, divided into 128 channels 1.8 mm wide by 1.5 cm in

length. Each channel has a high and low gain digitization path, which allow for energy measurements from a single MIP up to full energy electromagnetic showers. The short distance along the minipad sensors is rotated by ninety degrees for alternating layers to provide a three-dimensional high resolution image of the developing electromagnetic shower.

The sensors are a joint development project between Yonsei University and Brookhaven National Laboratory and will be produced at ETRI in Korea. The design after going through five development/R&D runs of the sensors is now highly advanced.

In addition to the sensors themselves, the Si micromodules consist of a sensor bonded to a dual-SVX readout card (ROC). The ROCs (designed by ISU and BNL) have been prototyped and Rev1 modules are being produced for testing. Each ROC has two SVX4 custom ASICs for digitization and readout (high and low gain channels). The ROC readout has been verified with the prototype modules populated with SVX 4.2b chips from a previous production. These chips have been produced by MOSIS/TSMC and have been wafer tested at Iowa State.

The micromodules for the MPC-EX plug into a "carrier board" – see Figure 2.3. Each carrier board has two readout chains of six micromodules. The carrier board is being designed by Iowa State, and a prototype is expected in June 2013. Because the SVX4s handle digitization and are read out in a serial "daisy chain" fashion, the FEM required to interface them to the PHENIX DAQ is relatively simple. A FEM design already existed for reading out prototype Si strip modules for another project, and the new MPC-EX FEM will build on this design.

During the summer of 2013 the MPC-EX group will place a collection of 25 MPC crystals in a test bean at FNAL. A Letter of Intent has been submitted to FNAL and we are awaiting confirmation on scheduling. The primary goal of this test beam will be to characterize the response of the MPC APDs to charged particles. Because the MPC APDs sit on the front of the detector they will be exposed to the partially developed shower when the MPC-EX is in place. Understanding the sensitivity of the APDs to charged particles will be important in understanding the overall operation of the combined MPC and MPC-EX detectors. Depending on the timing of the test beam and the availability of sensor micromodules a secondary goal of this effort will involve a partial preshower detector in front of the MPC crystal stack.

The MPC-EX group intends to install between 2–4 carrier boards (24–48 sensor micromodules) in front of one of the MPC arms prior to Run-14. This will likely be installed as four layers above or below the beamline, but a final configuration has not been decided at this time. The purpose of this installation will be to gain experience with the detector operating in the PHENIX muon piston so that systems integration issues such as noise, temperature stability, etc., can be investigated and solved prior to the full installation for Run-15. At the present time we see no technical or schedule impediment to installing both MPC-EX arms in time for RHIC Run-15.

2.4 Muon trigger system

The PHENIX *W* physics program relies on upgrades of the muon system in order to be able to trigger on high momentum muons. This system has two principal components which were commissioned before and during 2012. Additional trigger cards for the front-end electronics of the muon tracking chambers (MuTr) provide the necessary capabilities to include the muon tracker information in the trigger chain (funded by the Japan Society for the Promotion of Science). Resistive plate chambers (RPC) in front of (RPC1) and behind (RPC3) the existing muon arm detectors combine additional track information with good timing resolution for the trigger system (funded by the U.S. National Science Foundation).

The Level-1 trigger decisions are based on matching of the high momentum MuTr tracks (SG1) with hits in the RPCs. Timing information from the RPCs is further used to reject beam backgrounds in the trigger decision and to connect the recorded event to the correct bunch crossing and, therefore to the correct beam polarization. The RPC3 system was installed and commissioned for Run-11. RPC1 was added during the shutdown in the summer of 2011 and commissioned in Run-12, but it wasn't included in the physics trigger in Run-12. The RPC1 trigger was commissioned during Run-12 U+U data taking following the 510 GeV $p+p$.

The total rejection power for the sum of the *W*-physics triggers is improved in Run-13 compared to that of Run-12 as shown in Figure 2.4, and the rejection power for Run-13 is well above that required to fit within the PHENIX data acquisition bandwidth limit ($\sim$ 2KHz) assigned for muon arm associated triggers. The success of this trigger upgrade has enabled a full sampling of the available $p+p$ @ 500 GeV delivered luminosity in Run-13. The *W* to μ and to *e* analyses from Run-13 are already underway with a Fast Production at the RHIC Computing Facility (RCF) and a focused analysis effort planned at RIKEN in Japan in July 2013.

2.5 Hadron-blind detector

The PHENIX Hadron Blind Detector (HBD) upgrade was designed to significantly improve the signal to background in the measurement of correlated electron pairs that are sensitive to many exciting physics effects in the quark-gluon plasma [15]. The HBD was installed in Run-07 for an engineering run. That experience drove changes in the detector assembly procedure, resulting in a much cleaner detector when the HBD was re-installed for successful physics data taking with $p+p$ collisions in Run-09 and Au+Au collisions at various energies in Run-10. The HBD was subsequently removed for installation in the same physical space of the silicon vertex detectors.

The dielectron analysis is particularly challenging due to the need to reject many sources of background and normalize the combinatorial background with great precision. Careful analysis work has resulted in a very accurate gain calibration needed to discriminate

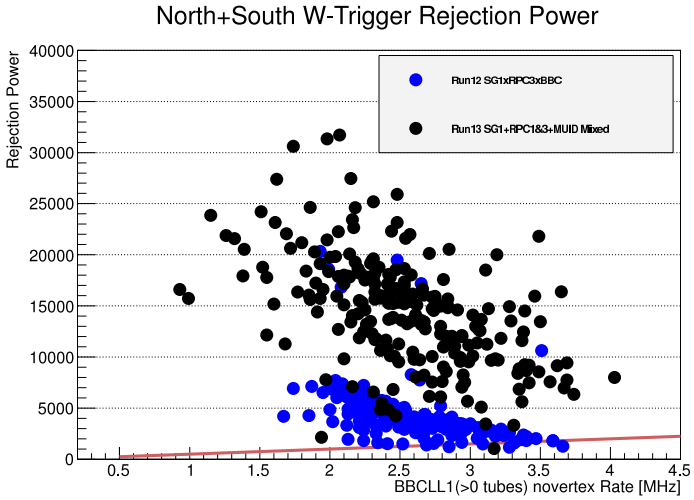

Figure 2.4: Total rejection power of combined 5 triggers dedicated for W-physics plotted as a function of BBC rate (proportional to luminosity). The total trigger rejection power for the W in Run-13 is compared with that achieved in Run-12. The red line shows the PHENIX bandwidth $\sim$ 2 kHz assigned for the muon arm associated triggers.

between one and two electron hits in the HBD. Gain changes due to geometrical variations of the hole size in the GEM foils are corrected for and time dependent variations are tracked. At this point the detector performance and alignment are very well understood.

In p+p as well as peripheral Au+Au collisions a simple cluster finding algorithm in the HBD can be used for efficient electron identification as well as for the rejection of the conversion electrons copiously produced in the back-plane of the HBD. This algorithm, requiring a minimum charge sum in a few pads around the projection point of an electron track onto the HBD, is not adequate for central or mid-central Au+Au collisions due to the large number of scintillation photons produced by charged particles traversing the CF_4 radiator gas. In order to still recognize the electron hits, an underlying event subtraction based on the average charge per cell is performed on an event-by-event basis and for each HBD module separately. The resulting performance is then limited by the fluctuations in the cell charge. A rejection of back-plane conversions of more than 90% (or rejection factor of 10) can be achieved while keeping a 90% electron efficiency from peripheral Au+Au up to 30–40% centrality. For a 90% rejection at higher centralities, the efficiency decreases and reaches values of 65% for the most central 0–10% bin.

This past year preliminary mass spectra measured with the HBD in p+p collisions and in peripheral (60–92%), semi-peripheral (40–60%) and semi-central (20–40%) Au+Au collisions at $\sqrt{s_{NN}} = 200$ GeV were presented [16], as shown in Figure 2.5. The p+p result is fully consistent with the previous PHENIX publication without the HBD [17]. In the most peripheral Au+Au bin the measured spectrum is in quite good agreement with the expected yield. For semi-peripheral and semi-central events there is a hint of a

small enhancement of the measured yield with respect to the cocktail that increases with centrality, both in the low-mass and the intermediate mass regions. However, no clear statement could be made given the very conservative uncertainties that were assigned at this preliminary stage.

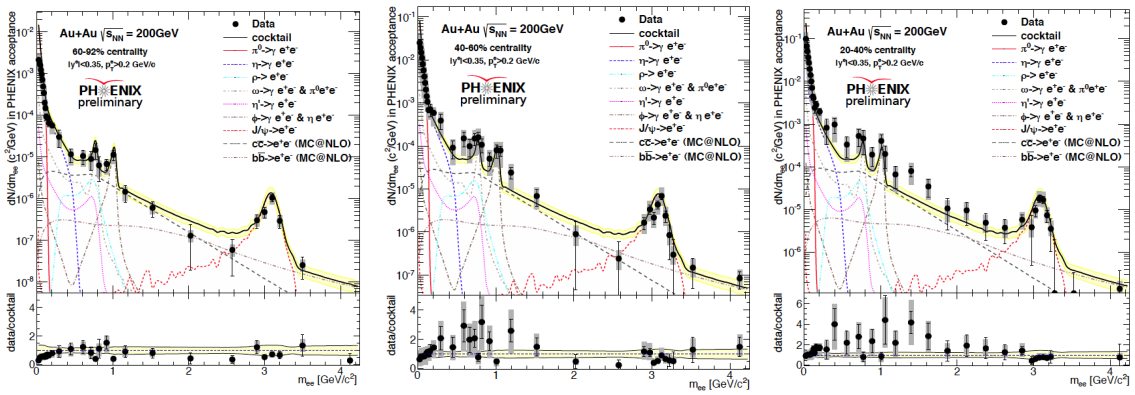

Figure 2.5: Invariant mass spectrum of e^+e^-pairs in Au+Au collisions at $\sqrt{s_{NN}} = 200$ GeV measured in the Run-10 with the HBD in three centrality bins. The data points show statistical (vertical bars) and systematic (shades) uncertainties separately. The data are compared to the expected yield from a cocktail of the known hadronic sources. The shaded band represents the systematic uncertainties of the cocktail. The bottom panel shows the data to cocktail ratio.

In the preliminary analysis, the background was subtracted in two separate steps. In the first step, the combinatorial background was subtracted using a mixed event technique. In the second step, the residual background of correlated pairs was subtracted using the residual like-sign spectra, corrected for the acceptance difference between $++$, $--$ and $+-$ pairs [15]. This approach could be used for the three centrality bins discussed above. However, for the two most central bins, the necessary accuracy in the acceptance correction could not be achieved (for central collisions, we required understanding of the background at the $\sim$0.1% level) and consequently reliable mass spectra could not be obtained.

Substantial improvements have been identified to allow for the dielectron physics extraction in the most central Au+Au collisions where the largest physics effects have been previously observed [15]. There is a better quantitative understanding of the normalization and different correlated components of the background. The event mixing techniques and kinematic range for normalizing mixed event have been optimized. Detailed simulations of cross pairs and jet contributions were developed and are currently being performed with high statistics in order to implement a source by source subtraction of the residual background (instead of subtracting the acceptance corrected like-sign residual spectra). In addition, much better hadron rejection is now achieved. This will mainly benefit the central collisions (for non-central collisions the hadron contamination is very small) and we expect the purity of the electron sample to rise from 80% to more than 90%.

The preliminary analysis was done using strong QA cuts. These are being relaxed in order to make use of most of the available statistics. In particular, the z-vertex cut is currently

restrictive, but that cut is being loosened. Other fiducial cuts used to homogenize the PHENIX detector response over large periods of time are removed and instead a run-by-run correction is implemented to account for the time variations of the detector acceptance. An increase of the e^+e^-pair yield of $\sim 40\%$ is expected as a result of these relaxed cuts.

We are now incorporating all the aforementioned changes and improvements into the analysis chain that will allow us to obtain raw mass spectra for all the centrality bins including the most central ones. We will then perform all the necessary simulations and corrections to obtain the absolutely normalized mass spectra within the PHENIX acceptance. We project that the basic analysis will be completed before the end of the year and we look forward to the physics results.

2.6 Other upgrades

There are several other upgrade projects besides those discussed in the previous sections that are making an impact on the PHENIX physics program. A few of these will be discussed here.

2.6.1 DAQ2010

The Data Acquisition and Trigger (DAQ2010) upgrade was implemented to handle the higher data throughput generated by the RHIC-II luminosity and the increased channel count of the VTX and FVTX detectors. The new detectors have approximately doubled the size of an average minimum bias Au+Au event. Nonetheless, with the data acquisition upgrades (such as the DCM II), the PHENIX DAQ has been able to maintain high livetime and event rate.

2.6.2 TOFW

The TOFW is a time-of-flight detector in the western half of the PHENIX central arm spectrometer. It is based on MRPCs and was intended to extend the π, K, p particle identification capabilities of PHENIX to higher transverse momentum. Figure 1.1 shows data from a recently submitted publication [4], providing an example of the extended PID capabilities of the TOFW.

2.6.3 MPC electronics

When it was first installed, the MPC electronics were based around an analog pipeline with digitization occurring only when a trigger was received. Prior to Run-12, those electronics

were replaced by readout electronics developed for the HBD. The significant difference is that these new electronics are based around a waveform digitizer and thus the entire readout and triggering chain is digital. The new capability for a Level-1 trigger decision based on fully digitized energy information has resulted in a significantly improved trigger rejection and physics sampling.

Chapter 3

Proposal for Run-14 and Run-15

In this section we provide details on the PHENIX collaboration beam use request, including the assumptions and inputs for luminosities and number of weeks for each request.

3.1 Accelerator performance and luminosity estimates

The physics performance evaluations in this document are based upon guidance provided by the Collider Accelerator Division (C-AD) as documented in Ref. [1]. Also necessary are projections for the PHENIX experiment performance in terms of uptime and trigger sampling. We use the following values based on metrics from the experimental running over the last three years.

- The PHENIX up time (the fraction of time when the beams are colliding that the PHENIX data acquisition is running and thus sampling physics) is 70%. This has been an area that PHENIX has placed particular emphasis on and observed consistent improvement.
- The PHENIX forward and barrel silicon vertex detectors have an optimal acceptance for collisions with z-vertex $|z| < 10$ cm. For other analyses in the central arm spectrometers not requiring the vertex detectors the acceptance is optimal for $|z| < 30$ cm. For the new MPC-EX forward measurements an even wider collision vertex range is utilized: $|z| < 40$ cm. We have labeled all physics projection integrated luminosities with the corresponding z-vertex range. Although the fraction of collisions within each selection varies somewhat with collision species, for these projections we consistently assume that 70% of all collisions are within $|z| < 40$ cm, 60% of all collisions are within $|z| < 30$ cm, and 30% of all collisions are within $|z| < 10$ cm.
- The PHENIX data acquisition livetime is quite high — typically better than 90%.

All of this information is utilized and the values quoted in the performance figures are in terms of sampled integrated luminosity by PHENIX within the specified z-vertex range.

3.2 Run-14 request for Au+Au @ 200 GeV

The PHENIX collaboration expects to collect our definitive heavy ion Au+Au data set for heavy quarks with the forward and barrel silicon detectors in Run-14. The original excitement of testing jet quenching energy loss scenarios with heavy quarks remains strong, and is only added to by the quest to answer whether low to modest transverse momentum charm and even beauty quarks thermalize in the quark-gluon plasma and take part in hydrodynamic flow. The integrated luminosity of the request 1.5 nb^{-1} within $|z| < 10$ cm (the equivalent of recording 10 billion Au+Au minimum bias events) is driven by the statistics requirement to make definitive heavy quark separation measurements over a broad transverse momentum and centrality range. In addition to the heavy quark measurements, we expect significant improvement in other measurement channels including for example in the J/ψ signal to background with the forward silicon vertex detector at forward rapidity [18] and a factor of 2.5 improvement on direct photon-hadron correlations [12].

The PHENIX silicon detectors enable the tagging of charm and beauty meson via the decay electron (midrapidity) or muon (forward rapidity). Over most of the transverse momentum range the data is collected via the Au+Au minimum bias trigger and the enormous data sample is achieved through the high bandwidth data acquisition system running at greater than 5 kHz. The accelerator projections with stochastic cooling very nearly saturate this bandwidth through the store for collisions within the silicon detector optimal acceptance of $|z| < 10$ cm. For very high transverse momentum electrons and photons we also enable selective Level-1 triggers.

The projected heavy flavor measurement in the forward silicon vertex detector (FVTX) is shown in Figure 3.1. Note that these nuclear modification measurements are shown with the projected statistics for the $p+p$ @ 200 GeV baseline as also requested in Run-14.

The midrapidity silicon vertex detector (VTX) collected a first Au+Au @ 200 GeV data set in Run-11. As detailed in the detector upgrade Section 2.2, this first running period for the VTX was at the start of an important learning curve. First results shown at the International Quark Matter Conference in 2012 [14] suffered from a lack of full unfolding in separating the charm and beauty contribution, which is critical at low transverse momentum, particularly if the heavy meson spectra are significantly modified. In Figure 3.2 we include updated physics projections for the VTX with the data sample achievable in Run-14.

The PHENIX collaboration has been working very hard towards an improved detector performance in Run-14 and a full unfolding procedure for publication of the electron measurements. As a demonstration with statistics comparable to that projected for Run-

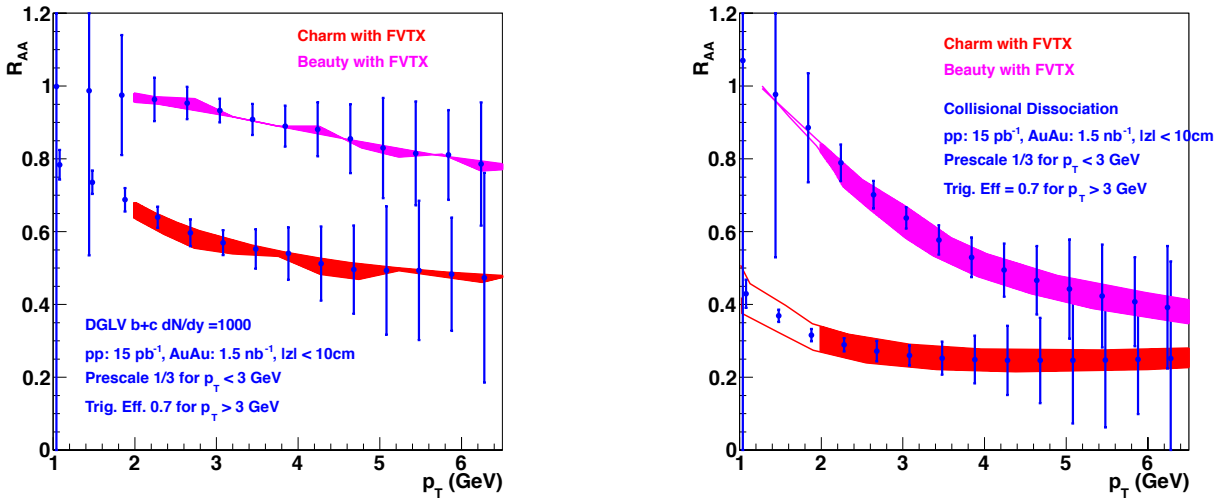

Figure 3.1: Simulation performance for the FVTX measurement of the nuclear modification factor for muons from beauty and charm decays as separated with displaced vertex measurements. The left panel corresponds to predictions from DGLV [19] and the right panel to predictions incorporating additional collisional dissociation processes [20].

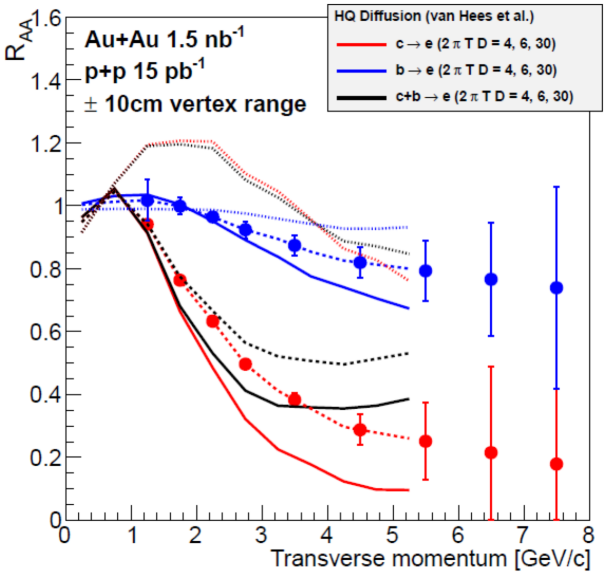

Figure 3.2: Simulated performance for the VTX measurement of the nuclear modification factor for electrons from beauty and charm decays as separated with displaced vertex measurements. These measurements are for the 0–10% central Au+Au collisions. Also shown are various heavy quark diffusion calculation results from van Hees *et al.* [21]

14, we have applied unfolding techniques to compute the parent D and B meson p_T distributions from electron DCA measurements simulated by PYTHIA. A transfer matrix

encoding the D and B to electron decay kinematics was modeled using default PYTHIA hadron momentum distributions. However, the simulated electron data were generated from a heavily modified sample, using R_{AA} values inspired by blast-wave fits to heavy flavor spectra [22]. Despite the independence of the decay model on this modification, both a Bayesian Markov Chain Monte Carlo algorithm (not shown) and a Generalized Singular Value Decomposition algorithm are able to consistently reproduce the modified parent distributions, as shown in Figure 3.3.

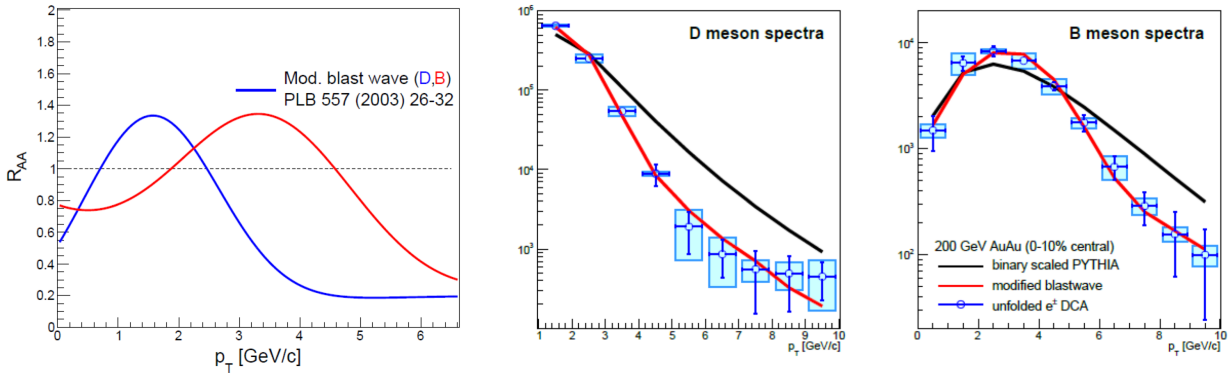

Figure 3.3: (left panel) Theory projection for D and B meson nuclear modification factors in a modified blast wave scenario [22]. (right panels) Using the modified blastwave scenario, generated comparable Run-14 statistics for fake data electron DCA distributions as a function of electron transverse momentum. The resulting unfolded distributions are shown as blue points with propagated variance (lines) and bias error from regularized unfolding (boxes).

3.3 Run-14 request for p+p @ 200 GeV with longitudinal polarization

As detailed in the previous section, this p+p @ 200 GeV request is important for the timely measurement of the baseline for the heavy quark modification measurements. The main driver for running with longitudinal polarization is the ability to significantly further constraint the gluon contribution to the proton spin. In the last year, the combined measurements of the PHENIX and STAR Collaborations combined with the DSSV theoretical effort have shown for the first time indications of a non-zero gluon contribution to the proton spin [2].

The challenge in such measurements in pushing the limits at the low-x (parton momentum fraction) end is to efficiently sample the luminosity with neutral pion triggers at low transverse momentum and control the systematic uncertainties. We have a detailed plan for the low threshold Electromagnetic Calorimeter triggers that enables a significantly greater constraint, even relative to the larger p+p @ 500 GeV data sets collected. The achieved and expected uncertainties from our 200 GeV program are shown in Figure 3.4,

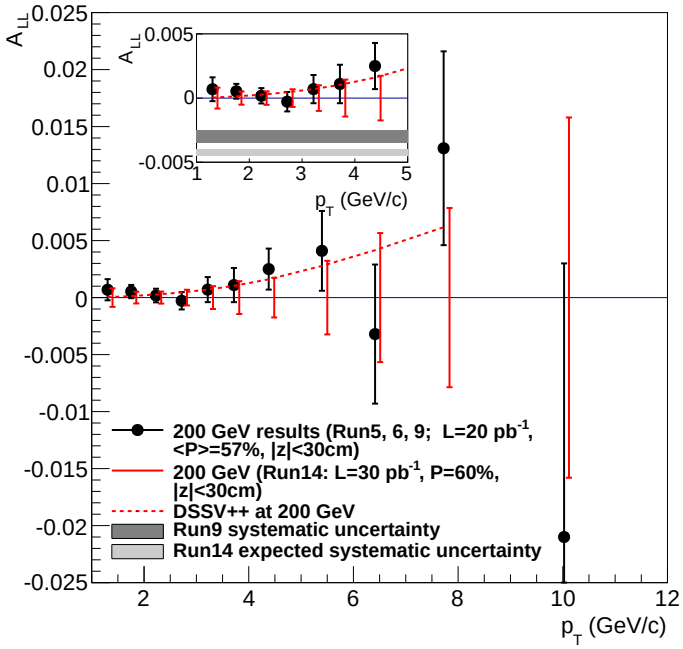

Figure 3.4: π^0 A_{LL} at $\sqrt{s} = 200$ GeV for the combined 2005–2009 RHIC runs, compared to the expected uncertainties for Run-14. The solid bands show the systematic uncertainty from relative luminosity.

along with a comparison to the theoretical expectations based on the DSSV^{++} [2] theoretical analysis. The figure shows that the additional data will double the statistics of the previous result used in the recent DSSV analysis. Further, the p_T correlated systematic uncertainty from relative luminosity in 2009 was twice that of the smallest statistical uncertainty. Since 2009, several studies, and better constraints on the transverse polarization component at PHENIX, have helped reduce this systematic uncertainty. In Run-14, we expect the systematic uncertainty to be reduced to a few times 10^{-4}. The relative impact of the 200 and 500 GeV programs is shown in Figure 3.5. The figure shows that the 200 GeV program has significantly greater power to constrain the gluon distribution for $0.01 < x_T < 0.04$, where $x_T = 2p_T/\sqrt{s}$.

Figure 3.6 relates to the forward A_{LL} measurement using the Muon Piston Calorimeter (MPC). The expected uncertainties and relative kinematic coverage between mid and forward rapidity are shown. The forward measurement samples lower values of Bjorken x, where the polarized gluon distribution has large uncertainties.

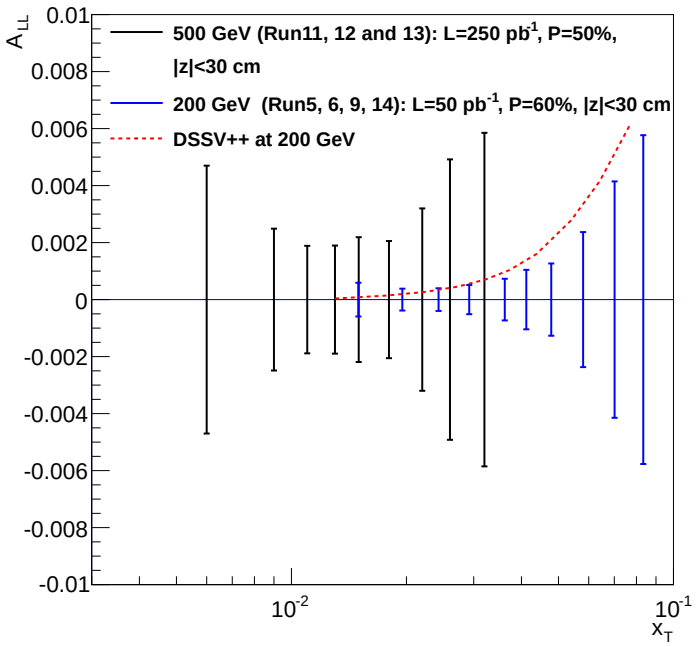

Figure 3.5: π^0 A_{LL} at $\sqrt{s} = 200$ GeV (blue) and $\sqrt{s} = 500$ GeV (black) as a function of x_T. At the same x_T, the 200 GeV data is more sensitive to the gluon helicity.

3.4 Run-15 request for $p+p$ @ 200 GeV with transverse polarization

The new capabilities of the MPC-EX upgrade and the interest in transverse spin physics drive our request for transversely polarized $p+p$ @ 200 GeV running. Even in the case that Run-14 does not fulfill our request for $p+p$ running with longitudinal polarization, we would request transverse polarization for $p+p$ in Run-15. The running also provides additional statistics for all heavy ion baseline measurements. The large transverse single-spin asymmetries observed in polarized $p+p$ collisions at RHIC are believed to be related to a combination of initial and final state effects that originate primarily in the valence region of the projectile nucleon, the Sivers or transversity distributions in the transverse-momentum dependent TMD approach, or parton correlations in a collinear factorized framework. While data in semi-inclusive deep-inelastic scattering has been used to constrain these effects, the situation is more complicated in $p+p$ collisions due to the presence of both strong initial and final-state corrections arising from the soft exchange of gluons. Existing measurements at forward rapidity at RHIC in transversely polarized $p+p$ collisions are limited to hadronic observables, and therefore sample a number of different partonic processes. In contrast, direct photon production at forward rapidity is dominated by the scattering of a valence quark from the polarized projectile off a low-x gluon in the unpolarized proton.

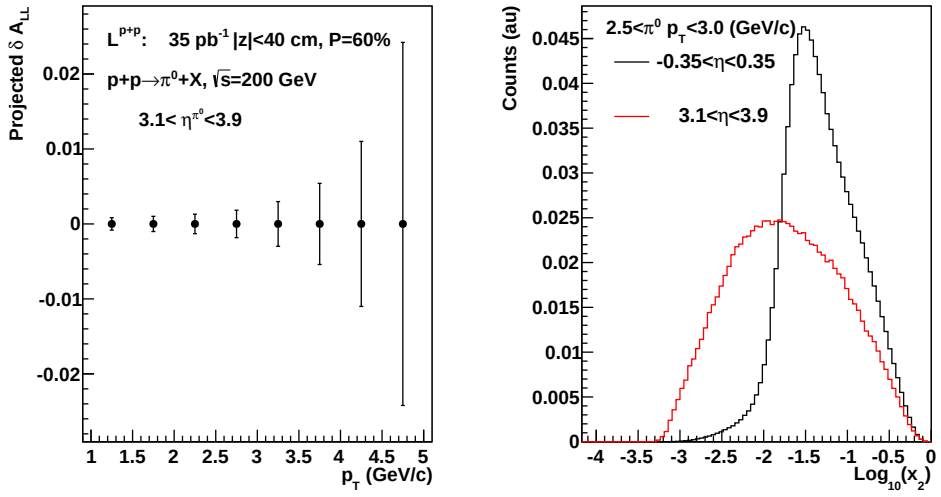

Figure 3.6: (left) Projected uncertainties for an A_{LL} measurement at forward rapidity using the MPC. (right) Results from a PYTHIA Monte-Carlo study on the Bjorken x ranges sampled at mid-rapidity (black) and at forward rapidity (red).

Prompt photons at forward rapidities are roughly an equal mix of direct photons and photons from the fragmentation of the scattered valence quark. Theoretical studies indicate that the contribution from transversity and a polarized fragmentation function is small so that the single spin asymmetry for fragmentation photons largely carries the same information about the initial state of the polarized nucleon and reinforces the asymmetry from direct photons. A measurement of the single spin asymmetry for prompt photons will shed light on the mechanisms that produce asymmetries in forward hadron production in polarized $p+p$ collisions, and their relationship to the spin asymmetries measured in semi-inclusive deep-inelastic scattering (SIDIS). Because prompt photons are sensitive to "initial state" effects, such as the Sivers function, the measurement of a prompt photon A_N directly addresses NSAC milestone HP13.

The expected measurement statistical precision from the MPC-EX measurement is shown in Figure 3.7, along with theory predictions from Kang *et al.* [23]. This figure includes contributions from direct and fragmentation photons, as well as the subtraction of the π^0 and η background asymmetries. The integrated luminosity request is driven by the requirement to make a definitive determination of the sign and pin down the magnitude at the $< 2\%$ level. The predicted sign of the asymmetry is different between extractions of the Sivers function from SIDIS data and the twist-3 quark-gluon correlation function extracted from RHIC asymmetries. Measurement of a prompt photon asymmetry at RHIC will provide valuable insight into the different QCD methodologies applied to calculate these asymmetries.

There are a number other measurements in transversely polarized $p+p$ collisions that can

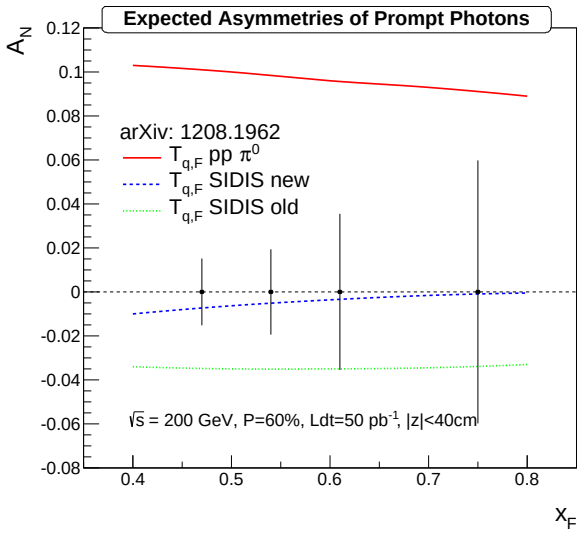

Figure 3.7: Projected sensitivity for the prompt photon single spin asymmetry with the MPC-EX assuming an integrated luminosity of 50 pb^{-1} and 60% beam polarization. The sensitivities are shown compared to calculations in the collinear factorized approach using a direct extraction of the quark-gluon correlation function from polarized p+p data (upper solid red curve), compared to the correlation function derived from SIDIS extractions (lower dotted and dashed curves).

also be made with a 50 pb^{-1} dataset, concurrent with the prompt photon measurement:

- Identified π^0 and η single spin asymmetries out to large transverse momentum (5–6 GeV/c)
- Measurement of the Interference Fragmentation Function (IFF) using hadron correlations (see Figure 3.8)
- Measurement of the contribution of the Collins fragmentation function to transverse single spin asymmetries through hadron correlations (both central + MPC as well as reconstruction of a jet axis in the MPC-EX)
- Measurement of heavy flavor A_N using single muons with improved background rejection with the FVTX detector (see Figure 3.9)

3.5 Run-15 request for p+Au @ 200 GeV with transverse polarization

There are a number of very exciting opportunities with polarized p+A collisions enabled by accelerator advances and the new detector capabilities in PHENIX since the last d+Au

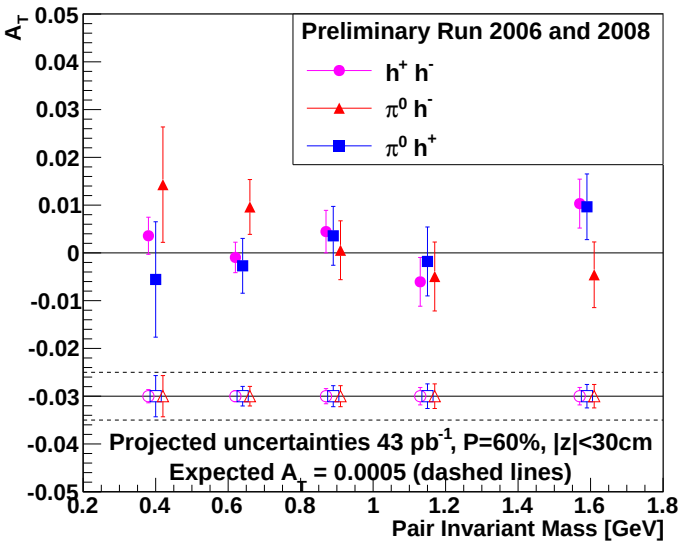

Figure 3.8: PHENIX preliminary results of interference fragmenation functions from Run-06 and Run-08. Shown are three different combinations of hadron pairs. Also shown are projections for the luminosity request in Run-15.

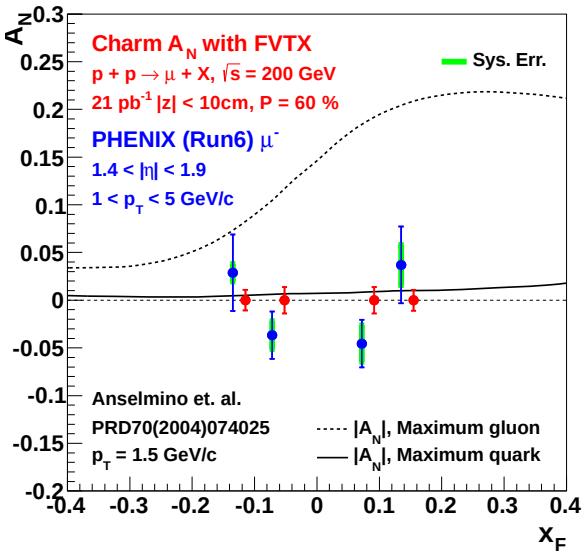

Figure 3.9: Single spin charm asymmetry, A_N, in transversely polarized p+p @ 200 GeV.

@ 200 GeV data taking in 2008. We highlight these opportunities with physics projection plots in the following subsections.

The highest priority for this set of colliding systems is for a high statistics p+Au @ 200 GeV data set with a PHENIX integrated luminosity of 150 nb^{-1} within the z-vertex range $|z| <$

40 cm (the optimal acceptance range for the MPC-EX). A key set of new observables utilize the polarization of the proton beam with a required 60% average transverse polarization. Since the accelerator has not run p+A systems before, we have estimated from other system ramp up times and the CA-D provided maximum luminosity projections that this requires four weeks of physics running. This will provide an excellent p+Au data set of a number of key observables.

We note that it might be beneficial to split the four weeks into two weeks of p+Au and two weeks of Au+p (i.e., reversing the beam directions). This was done with a two day turnaround for p+Pb to Pb+p running at the LHC. Comparing observables after swapping the p-going and Au-going directions provides a very useful way to understand and reduce systematic uncertainties in the measurement. We seek input from CA-D on the possible switching time and the implications on the delivered luminosities.

We highlight below the great utility in having comparable statistical precision measurements in p+Si and p+Cu systems, each of which requires two weeks of physics running. We note that the choice of lightest ion — listed here as Si — is still under some discussion in terms of whether an even lighter ion such as carbon might be better.

We then detail how a short, one week each, run of d+Au and ^{3}He+Au with the full suite of new detectors available may shine light on the physics of possible flow in such small systems.

3.5.1 Polarized p+A: a unique test of saturation physics

The prospect of unique transverse polarized protons colliding with nuclei has generated a great deal of interest in the community — see the recent BNL-LANL-RBRC workshop talks for more details [24].

The MPC-EX enables an exciting new measurement proposed by Kang and Yuan [25]. It is predicted that the ratio of single spin asymmetries for neutral pions in p+A collisions to that in p+p collisions as a function of transverse momentum will be sensitive to the ratio of saturation scales the two systems, with the ratio suppressed below one when $p_T < Q_{\rm sat}^A$. A measurement of the asymmetry ratio as a function of transverse momentum for different nuclear species will elucidate if a saturation mechanism is a correct description of the underlying physics at low-x, and characterize its A dependence. It should be noted that while this measurement borrows a technique from spin physics, the underlying physics measurement is directly related to cold nuclear matter. This represents a completely unique utilization of the excellent RHIC accelerator complex. Projected uncertainties with the requests p+Au and p+p @ 200 GeV transversely polarized running are shown in Figure 3.10. The addition of comparable statistical and systematic precision data in p+Cu and p+Si allow for a complete mapping out of this phenomenon.

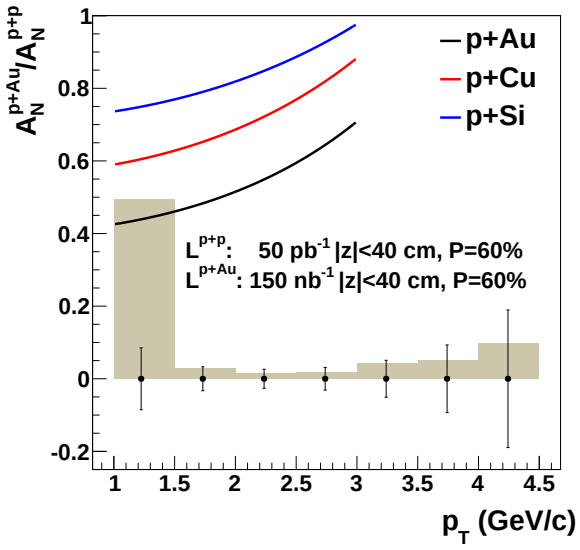

Figure 3.10: Shown are the projected statistical and systematic uncertainties for the requested polarized p+Au and p+p @ 200 GeV running. The colored curves represent a schematic expectation from the model of Kang and Yuan and apply for transverse momentum values below the saturation scale. These curves follow the functional form with the assumption that $Q_{\rm sat} = 1$ GeV/c and $Q_{\rm sat}^A = A^{1/3} Q_{\rm sat}$, plus a delta parameter related to the form of the Collins FF. The mapping out of the p_T and A dependence is thus very important.

3.5.2 Constraining the gluon nuclear PDF

One of the main physics goals of the MPC-EX is the characterization of the gluon distribution in nuclei at low-x. It has been known for some time that low-x gluons in nuclei are suppressed at small-x ($x \sim 10^{-3}$) compared to in protons, but the magnitude of this suppression is poorly constrained by existing experimental data. It has been conjectured that at low-x in the nucleus the gluon density saturates below a scale $Q_{\rm sat}$, forming a universal state known as the Color Glass Condensate. The existence of such a state would tame the rapid growth of the gluon PDF indicated by data from HERA DIS experiments, and there are tantalizing hints from RHIC d+Au collisions that such a state may be accessible at RHIC. Understanding the gluon distribution at low-x in nuclei is critical to a complete understanding of the formation and evolution of the quark-gluon plasma in heavy-ion collisions.

Current probes of low-x at RHIC have relied on hadronic probes, which average over many partonic processes and only partially access the gluon distribution in nuclei. Effects of shadowing and anti-shadowing are clear from the PHENIX measurements to date of quarkonia and open heavy flavor leptons in d+Au collisions; however, that does not allow for a precision quantification. In contrast, prompt photon production at forward rapidities is dominated by q+g scattering in leading order, and is optimally sensitive to the

gluon distribution. The MPC-EX will measure prompt photons in p+p and p+A collisions (with A = Au, Cu, and possible Si and C) for $p_T > 3$ GeV/c to extract the ratio R_{pA}. This measurement will provide constraints on existing models of the gluon distribution at low-x, such as the EPS09 nuclear PDFs [26]. The distribution of the number of binary collisions for each of these target nuclei calculated with Monte-Carlo Glauber is shown in Figure 3.11.

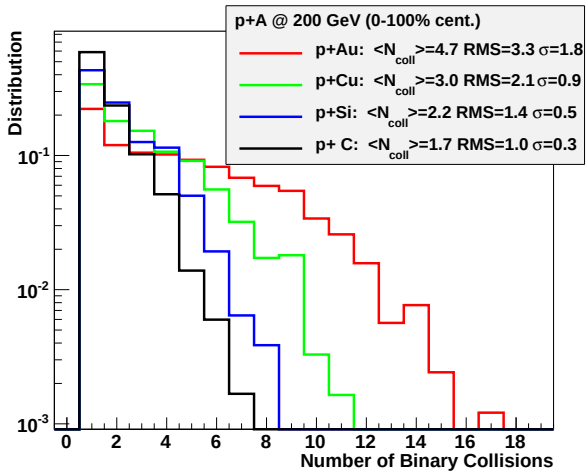

Figure 3.11: Distribution of the number of binary collisions calculated in a Glauber Monte-Carlo for p+A with various nuclear targets.

For the requested data samples, we have projections for the statistical and systematic uncertainties on the direct photon measurement in p+A and p+p @ 200 GeV. To gauge the constraining power of these measurements on the gluon nuclear parton distribution function, we consider the suite of EPS09 nPDFs. We carry out a global fit and find the one and two standard deviation consistency bands. Shown in Figure 3.12 is the full set of current EPS09 gluon nPDFs as a function of x in Au, Cu, Si nuclei. Then highlighted in dark and light blue are the one and two standard deviation constraints from this direct photon MPC-EX measurement.

Additional constraints with charm and beauty production at forward and backward rapidity with the forward silicon vertex detector (FVTX) allow for consistency checks. The projected measurements from the FVTX with a fully unfolded flavor separation are shown in Figure 3.13. These measurements, along with comparable ones at midrapidty with the VTX, also provide a crucial baseline for the A+A heavy flavor results — in particular with constraints on the Cronin effect and initial state parton energy loss.

Heavy quarkonia measurements in d+Au collisions have proven challenging to describe in terms of initial state nuclear modified parton distribution functions (nPDFs) and a simple nuclear break-up cross section [8, 27]. Extending these results to measurements in p+A collisions with various nuclear targets A will add key independent checks on the geometric dependencies. Shown in Figure 3.14 are the projected uncertainties for J/ψ measurements

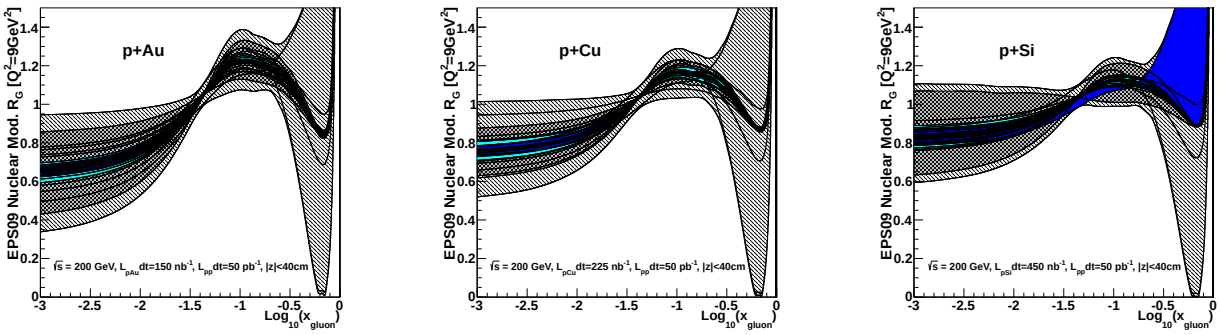

Figure 3.12: EPS09 nuclear parton distribution functions for gluons in Au, Cu, Si nuclei from left to right. The grey range shows the current band consistent with existing data. The dark blue and light blue bands show the one and two standard deviation constraints from the direct photon measurements proposed here.

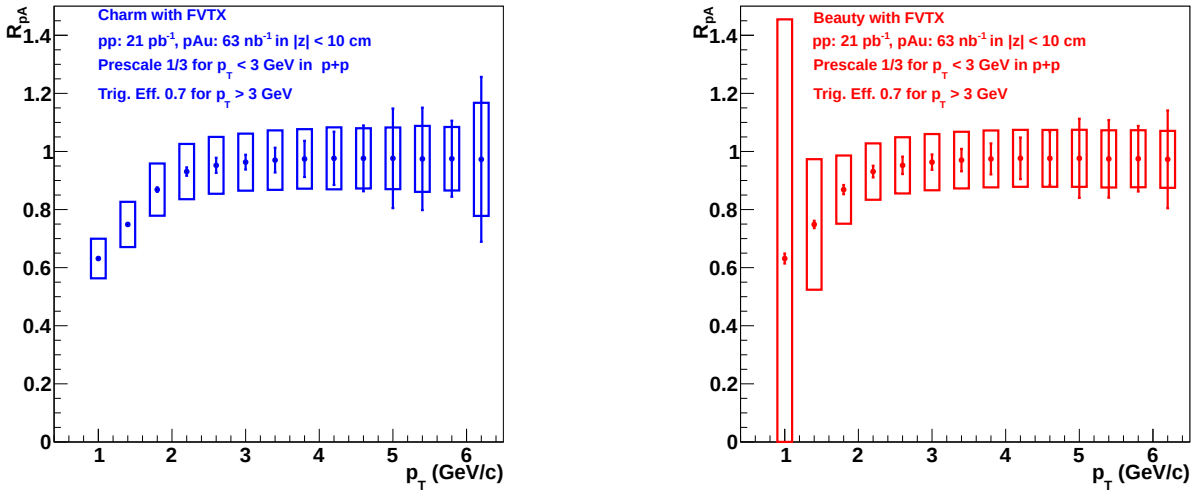

Figure 3.13: Projected uncertainties for R_{pA} for open charm (left) and open beauty (right) via the measurement of single muons with displaced verticies detected with the FVTX. The open boxes are systematic uncertainties that include contributions from the unfolding of the two heavy flavor components.

for four different possible nuclear targets for the proposed integrated luminosities.

The momentum resolution improvement in the muon arms with the addition of the FVTX provides for the first time the ability to measure the ψ' at forward and backward rapidities. Figure 3.14 (right panel) shows the ψ' projected uncertainties. The centrality dependence of the ψ' as a function of rapidity will be a key test of models of charmonium production at different time scales and gluon densities [28].

One key item on all of these measurements to note is the emphasis on the geometry dependence. For example, nuclear modified PDFs are to date largely constrained from

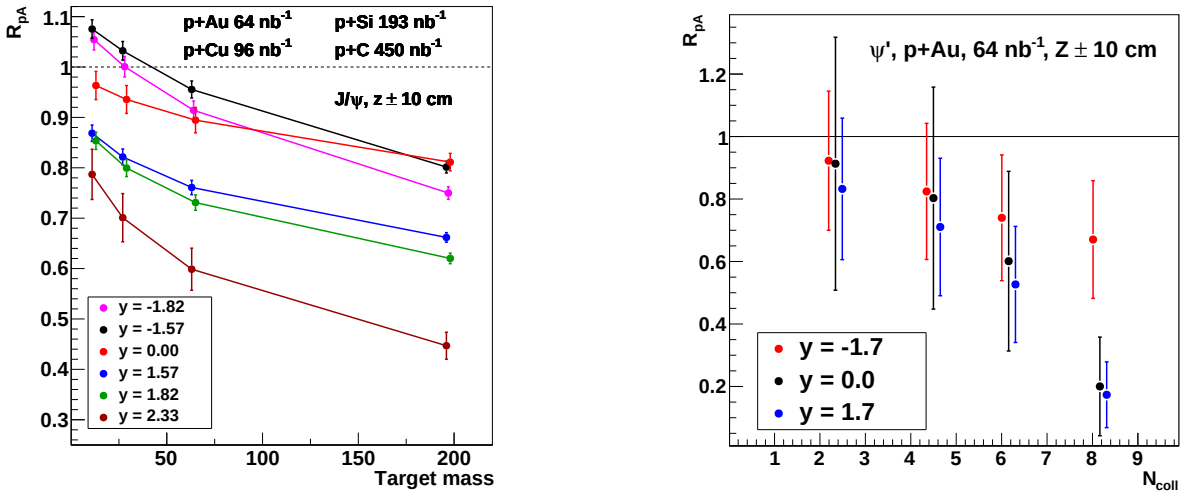

Figure 3.14: (left) Projected uncertainties for J/ψ R_{pA} and the possible nuclear and rapidity dependence from modeling of the d+Au measurements. (right) Projected uncertainties for the ψ' R_{pAu} at different rapidities from 64 pb^{-1}.

deep inelastic scattering from nuclei and thus average over the entire nucleus. Thus far, RHIC results have selected different nuclear densities via centrality selection in d+Au collisions. These result in quantified systematic uncertainties, though for the highest transverse momentum jet and neutral pion results additional autocorrelations with the centrality selections are under study (as shown earlier in Figure 1.5). The ability to check these nuclear dependencies with minimum bias p+A with different nuclei is critical for pinning down how these effects depend on the nuclear density. These dependencies are a key to unlocking the underlying physics. As one specific example, a two week p+Si run will allow for a better statistics measurement of the nominal physics of neutral pions and jets than the peripheral selection d+Au result.

3.5.3 Unique probes of geometry with d+Au and ^{3}He+Au

The long-range rapidity correlations observed at the LHC in high multiplicity p+p and p+Pb collisions and most recently in RHIC d+Au collisions have sparked a great deal of physics discussion. Are these correlations the result of glasma diagrams within a Color Glass Condensate picture? Are they the result of hydrodynamic expansion or non-equilibrium interactions? How do they relate to the initial geometry and the time evolution of the medium? Does a flow like mechanism in such small systems challenge the paradigm of perfect fluidity in A+A collisions or provide additional constraints on the underlying mechanisms? The lever arm from comparing RHIC and LHC results helps to answer these questions. However, at RHIC we also have the opportunity to tune the geometry uniquely to definitively test the fundamentals behind many of these questions.

The correlations are predominantly with low momentum particles and thus one requires a large minimum bias data set. The large PHENIX data acquisition bandwidth would allow an excellent measurement in d+Au and ^{3}He+Au with one week of running for each with a relatively low luminosity requirement. The new PHENIX detectors, not available during the earlier Run-08 d+Au run, including the large tracking coverage VTX, FVTX, and the new MPC-EX would make these an excellent data set for these studies with over 1 billion events in each system, and more in p+Au with the running detailed before.

The projected luminosities (store average) for d+Au and ^{3}He+Au are 28×10^{28} and 5×10^{28} cm^{-2}s^{-1} respectively. For these measurements, only a tiny fraction of that luminosity is required to saturate the minimum bias data acquisition bandwidth and achieve these one billion event data sets.

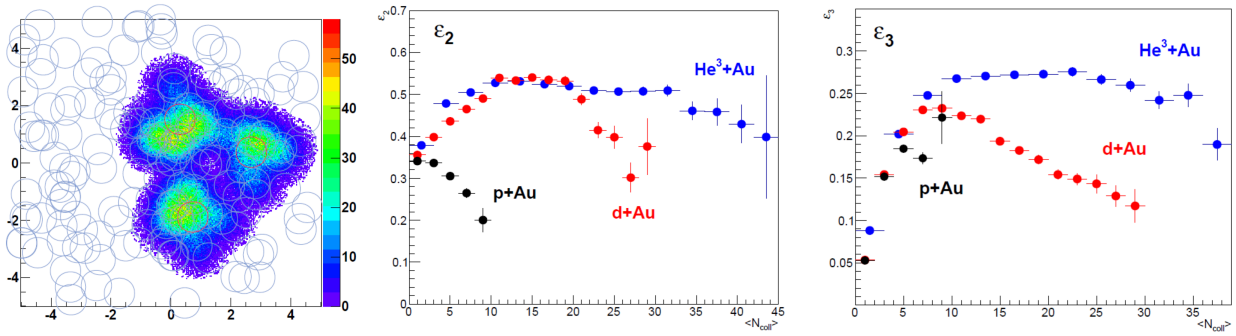

Figure 3.15: left) Monte Carlo Glauber event display of a single ^{3}He+Au event and the energy deposit. The nucleon participant energy is distributed as a Gaussian with $\sigma = 0.4$ fm. (middle and right) Monte Carlo Glauber mean ε_2 (middle) and ε_3 (right) for p+Au , d+Au, ^{3}He+Au collisions as a function of the number of binary collisions. The spatial moments are calculated using the same Gaussian smearing.

Just as the d+Au collisions have a significant intrinsic ε_2 (elliptical shape), the ^{3}He+Au collisions have a significant intrinsic ε_3 (triangular shape). The question of whether these two or three hotspots in deposited energy connect during the time evolution and result in significant v_2 and v_3 is what these measurements can definitively answer. In Figure 3.15 we show an example single ^{3}He+Au display with the energy deposit distribution assuming Monte Carlo Glauber with smearing around each participating nucleon with a Gaussian width of 0.4 fm. We also show the average ε_2 and ε_3 as a function of the number of collisions for all three systems. Note that we are working with James Shepard (Colorado) and David Dean (ORNL) for a full 3-body model of the ^{3}He case.

The exact total running time for all these related p+A, d+A, ^{3}He+A requests depends on how quickly the accelerator is able to achieve the p+Au projected luminosities and switching time between species. The prioritization of running after the p+Au @ 200 GeV running is something we expect to be further informed over the next year from new RHIC and LHC results and rapidly progressing theoretical developments.

Appendix A

Beam use proposal charge

Dear RHIC Collaborations:

In order to allow the RHIC-AGS PAC members sufficient time to prepare for the PAC meeting on June 11-12, 2013, the final version of the annual beam use proposals from the RHIC collaborations will be due on May 28, 2013, the day after Memorial Day. In order to permit Laboratory feedback before the proposals are finalized, I request that you send me a draft version of the beam use proposal one week before the submission deadline, no later than May 21.

The proposals should describe and justify which beam operations you would like to see during the 2014 and 2015 runs, which are currently planned as 22 week runs. Because funding levels for FY14 and FY15 are still unknown, you should also present plans for shorter runs of 15 weeks in each year. As usual, the beam use proposal should also give a brief review of recent published results and an early assessment of the success of Run-13.

Please send the proposals in electronic form to Peter Yamin, with copies to me, David Lissauer, Tom Ludlam, and Thomas Roser.

Thanks in advance for your cooperation in this important matter.

Best regards

Berndt

Bibliography

[1] C-AD Run-14 and Run-15 Projection Document (provided by W. Fischer). URL: http://www.rhichome.bnl.gov/RHIC/Runs/RhicProjections.pdf. (document), 3.1

[2] E. C. Aschenauer, A. Bazilevsky, K. Boyle, K. O. Eyser, R. Fatemi, et al. The RHIC Spin Program: Achievements and Future Opportunities. 2013. arXiv:1304.0079. (document), 1.4, 3.3, 3.3

[3] C. Aidala, N.N. Ajitanand, Y. Akiba, Y. Akiba, R. Akimoto, et al. sPHENIX: An Upgrade Concept from the PHENIX Collaboration. 2012. arXiv:1207.6378. (document)

[4] A. Adare et al. Spectra and ratios of identified particles in Au+Au and d+Au collisions at $\sqrt{s_{NN}} = 200$ GeV. 2013. arXiv:1304.3410. 1.1, 2.6.2

[5] A. Adare et al. Quadrupole anisotropy in dihadron azimuthal correlations in central d+Au collisions at $\sqrt{s_{NN}} = 200$ GeV. *Phys.Rev.Lett.*, 2013. arXiv:1303.1794. 1.1

[6] A. Bzdak, B. Schenke, P. Tribedy, and R. Venugopalan. Initial state geometry and the role of hydrodynamics in proton-proton, proton-nucleus and deuteron-nucleus collisions. 2013. arXiv:1304.3403. 1.1, 1.2

[7] Piotr Bozek. Collective flow in p-Pb and d-Pd collisions at TeV energies. *Phys.Rev.*, C85:014911, 2012. arXiv:1112.0915, doi:10.1103/PhysRevC.85.014911. 1.2

[8] A. Adare et al. Transverse-Momentum Dependence of the J/ψ Nuclear Modification in d+Au Collisions at $\sqrt{s_{NN}}$=200 GeV. 2012. arXiv:1204.0777. 1.1, 3.5.2

[9] A. Adare et al. $\Upsilon(1S + 2S + 3S)$ production in d+Au and p+p collisions at $\sqrt{s_{NN}} =$ 200 GeV and cold-nuclear matter effects. *Phys.Rev.Lett.*, 109:242301, 2012. arXiv:1211.4017, doi:10.1103/PhysRevLett.109.242301. 1.1

[10] A. Adare, S.S. Adler, S. Afanasiev, C. Aidala, N.N. Ajitanand, et al. Direct photon production in d+Au collisions at $\sqrt{s_{NN}} = 200$ GeV. 2012. arXiv:1208.1234. 1.1

[11] A. Adare et al. Cold-nuclear-matter effcts on heavy-quark production in d+Au collisions at $\sqrt{s_{NN}} = 200$ GeV. 2012. arXiv:1208.1293. 1.1

[12] A. Adare et al. Medium modification of jet fragmentation in Au+Au collisions at $\sqrt{s_{NN}} = 200$ GeV measured in direct photon-hadron correlations. 2012. arXiv:1212.3323. 1.3, 3.2

[13] A. Adare et al. Measurement of bottom versus charm as a function of transverse momentum with electron-hadron correlations in $p+p$ collisions at $\sqrt{s} = 200\,\mathrm{GeV}$. *Phys. Rev. Lett.*, 103:082002, 2009. arXiv:0903.4851, doi:10.1103/PhysRevLett.103.082002. 1.3, 1.9

[14] R. Nouicer. Probing hot and dense matter with charm and bottom measurements with PHENIX VTX tracker. 2012. arXiv:1212.3291. 1.3, 3.2

[15] A. Adare et al. Detailed measurement of the e^+e^- pair continuum in $p+p$ and Au+Au collisions at $\sqrt{s_{NN}} = 200\,\mathrm{GeV}$ and implications for direct photon production. *Phys. Rev.*, C81:034911, 2010. arXiv:0912.0244, doi:10.1103/PhysRevC.81.034911. 2.5, 2.5

[16] I. Tserruya. Photons and low-mass dileptons: results from PHENIX. 2012. arXiv:1211.6002. 2.5

[17] A. Adare et al. Dilepton mass spectra in $p+p$ collisions at $\sqrt{s} = 200\,\mathrm{GeV}$ and the contribution from open charm. *Phys.Lett.*, B670:313–320, 2009. arXiv:0802.0050, doi:10.1016/j.physletb.2008.10.064. 2.5

[18] A. Adare et al. J/ψ suppression at forward rapidity in Au+Au collisions at $\sqrt{s_{NN}} = 39$ and 62.4 GeV. *Phys.Rev.*, C86:064901, 2012. arXiv:1208.2251, doi:10.1103/PhysRevC.86.064901. 3.2

[19] M. Djordjevic, M. Gyulassy, R. Vogt, and S. Wicks. Influence of bottom quark jet quenching on single electron tomography of Au+Au. *Phys. Lett.*, B632:81–86, 2006. arXiv:nucl-th/0507019, doi:10.1016/j.physletb.2005.09.087. 3.1

[20] A. Adil and I. Vitev. Collisional dissociation of heavy mesons in dense QCD matter. *Phys. Lett.*, B649:139–146, 2007. arXiv:hep-ph/0611109, doi:10.1016/j.physletb.2007.03.050. 3.1

[21] H. van Hees et al. private communication. 3.2

[22] S. Batsouli, S. Kelly, M. Gyulassy, and J.L. Nagle. Does the charm flow at RHIC? *Phys.Lett.*, B557:26–32, 2003. arXiv:nucl-th/0212068, doi:10.1016/S0370-2693(03)00175-8. 3.2, 3.3

[23] L. Gamberg and Z.-B. Kang. Single transverse spin asymmetry of prompt photon production. *Phys.Lett.*, B718:181–188, 2012. arXiv:1208.1962, doi:10.1016/j.physletb.2012.10.002. 3.4

[24] The Physics of p+A Collisions at RHIC. https://indico.bnl.gov/conferenceDisplay.py?ovw=True&confId=553, January 2013. 3.5.1

[25] Zhong-Bo Kang and Feng Yuan. Single Spin Asymmetry Scaling in the Forward Rapidity Region at RHIC. *Phys.Rev.*, D84:034019, 2011. arXiv:1106.1375, doi:10.1103/PhysRevD.84.034019. 3.5.1

[26] K. Eskola, H. Paukkunen, and C. Salgado. EPS09: a new generation of NLO and LO nuclear parton distribution functions. *JHEP*, 04:065, 2009. arXiv:0902.4154, doi:10.1088/1126-6708/2009/04/065. 3.5.2

[27] A. Adare et al. Cold Nuclear Matter Effects on J/ψ Yields as a Function of Rapidity and Nuclear Geometry in Deuteron-Gold Collisions at $\sqrt{s_{NN}} = 200$ GeV. *Phys.Rev.Lett.*, 107:142301, 2011. arXiv:1010.1246, doi:10.1103/PhysRevLett.107.142301. 3.5.2

[28] Francois Arleo and Stephane Peigne. Heavy-quarkonium suppression in p-A collisions from parton energy loss in cold QCD matter. *JHEP*, 1303:122, 2013. arXiv:1212.0434, doi:10.1007/JHEP03(2013)122. 3.5.2